14986 - Physics-Based Model for Online Fault Detection in Autonomous Cryogenic Loading System

Vadim Smelyanskiy, Dmitry Luchinsky, Ekaterina Ponizhovskaya, Slava Osipov, Halyna Hafiychuk, Barbara Brown, and Anna Patterson-Hine

Dr. Vadim Smelyanskiy, vadim.n.smelyanskiy@nasa.gov
Integrated Product Team, NASA Ames Research Center

PHYSICS-BASED MODELING IN DESIGN & DEVELOPMENT NOV 2012

Contents

- Introduction
- Methodology
- Model Description
- Fault detection in transfer line
- Heat and mass leaks in the vehicle tank
- Work in progress

Loading Operation

Characteristic scales: L, D, d, Δt_P.
Flow rates: chilldown, reduced fill, fast fill, replenish
Fill time: T_{chill}, T_{red}, T_{fast}, T_{rep}
Total volume: V_{chill}, V_{red}, V_{fast}, V_{rep}

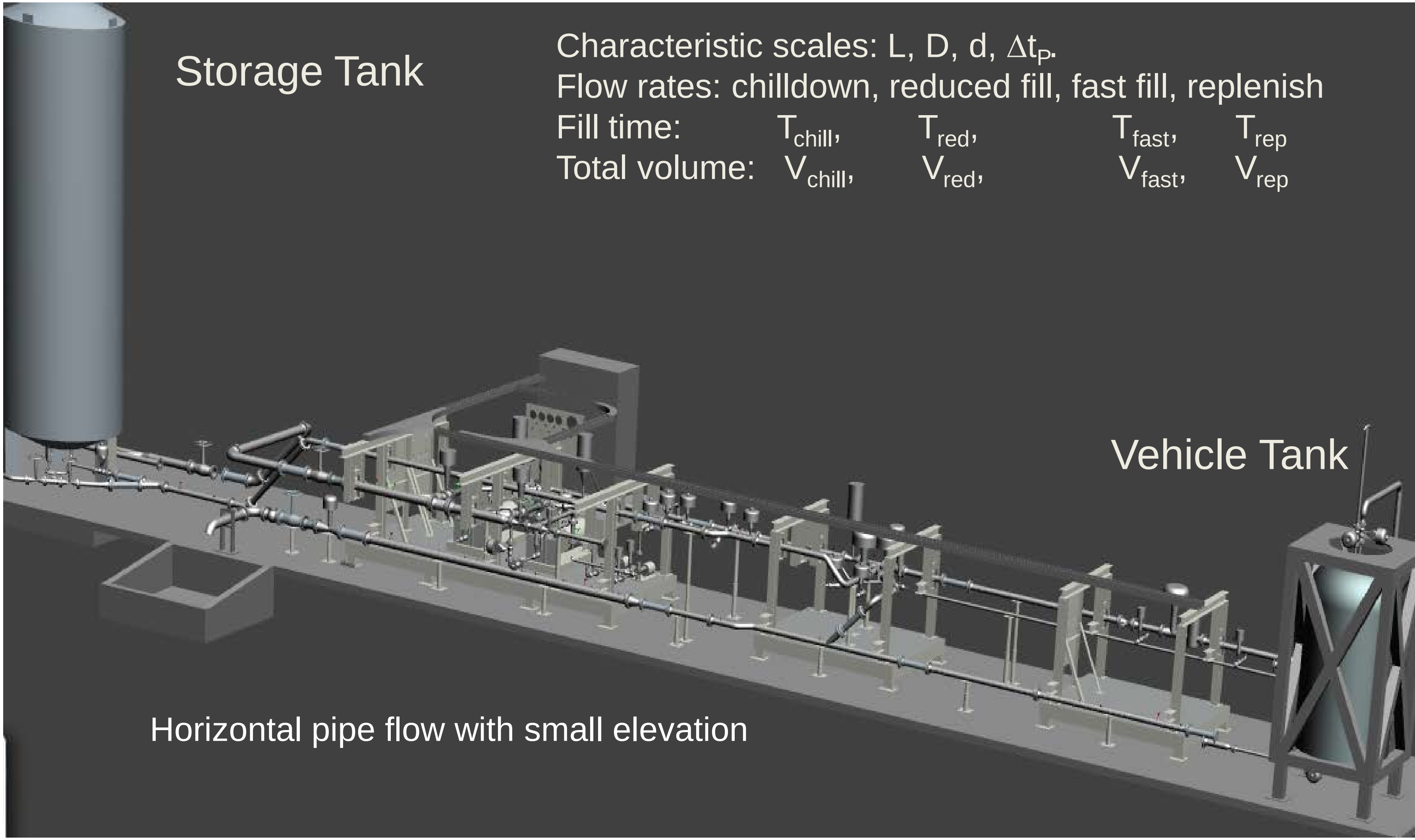

Horizontal pipe flow with small elevation

Typical Signals Measured During Loading

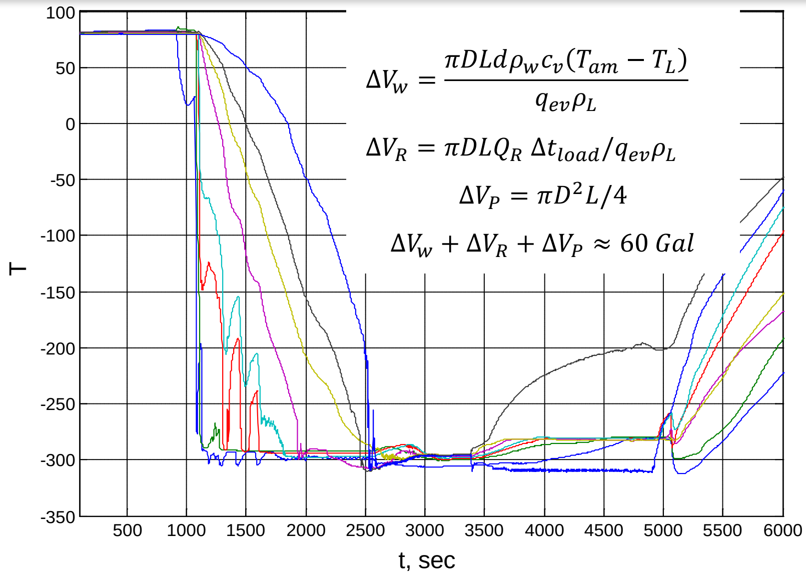

$$\Delta V_w = \frac{\pi D L d \rho_w c_v (T_{am} - T_L)}{q_{ev}\rho_L}$$

$$\Delta V_R = \pi D L Q_R \, \Delta t_{load} / q_{ev}\rho_L$$

$$\Delta V_P = \pi D^2 L/4$$

$$\Delta V_w + \Delta V_R + \Delta V_P \approx 60 \; Gal$$

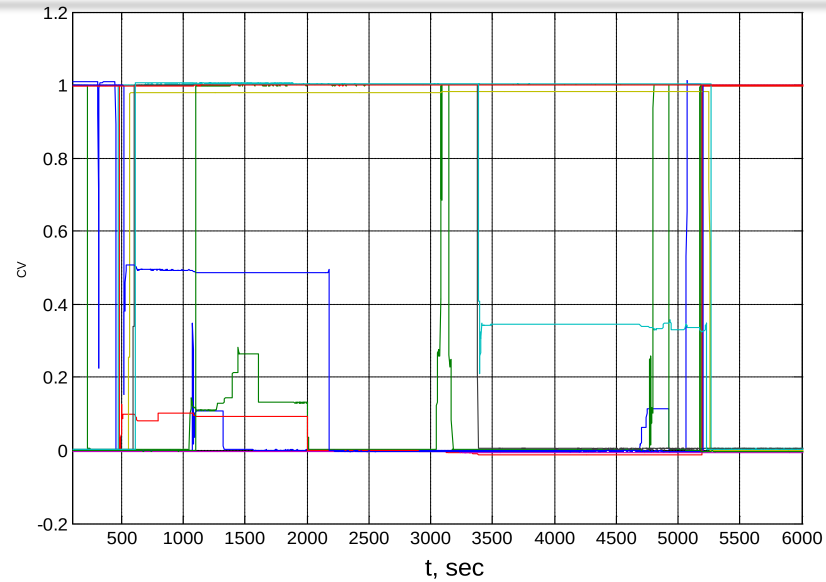

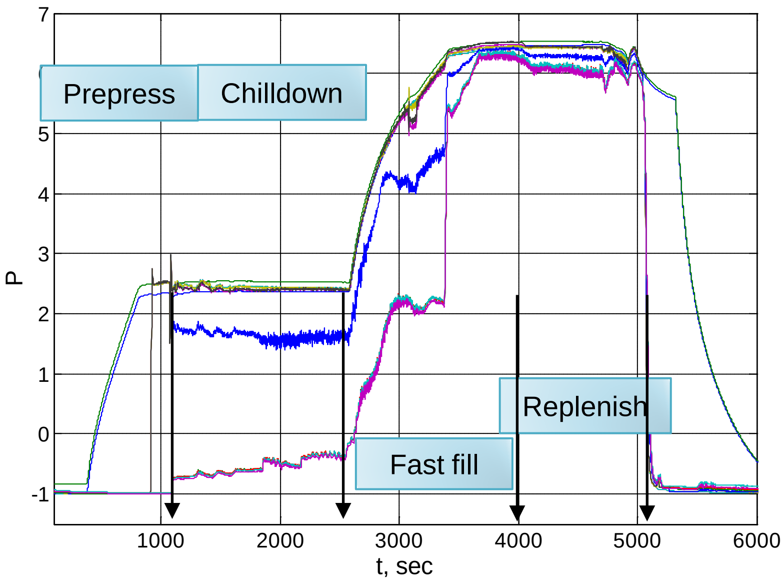

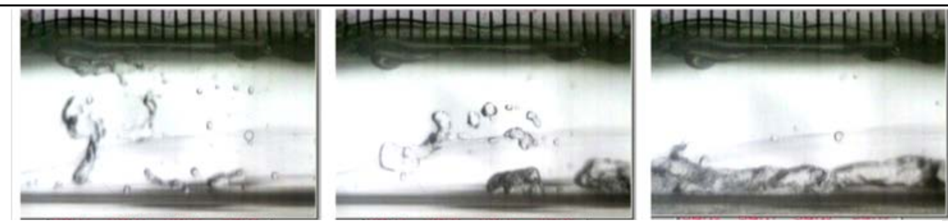

K. Yuan, Yan Ji, J.N. Chung, “Cryogenic chilldown process under low flow rates”, IGHMT, 50 (2007) 4011–4022

Complexity of the cryogenic loading operations is related to:

- Strongly non-equilibrium non-steady flow
- Childown
- Multiple fault regimes including mass and heat leaks
- Active control

Earlier Research

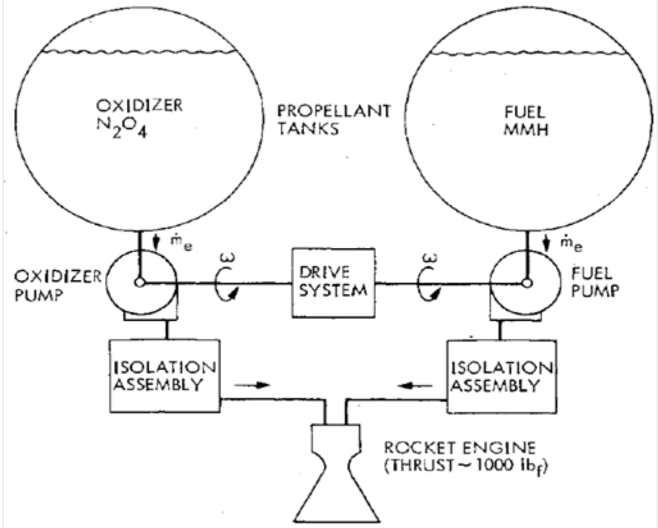

Fig. 1 Pump-fed propulsion system schematic drawing.

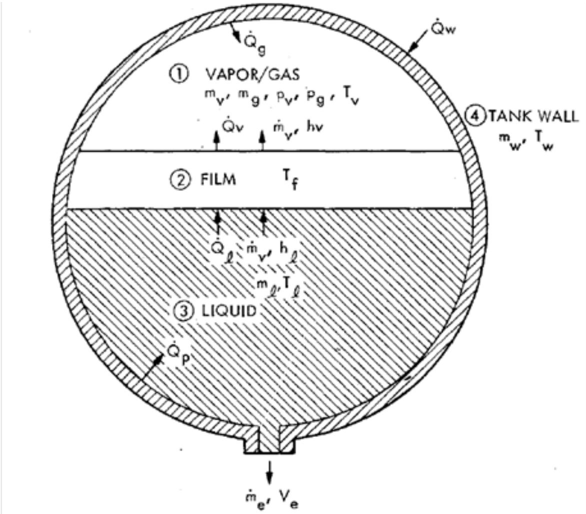

Fig. 2 Sketch of propellant supply tank showing control volumes.

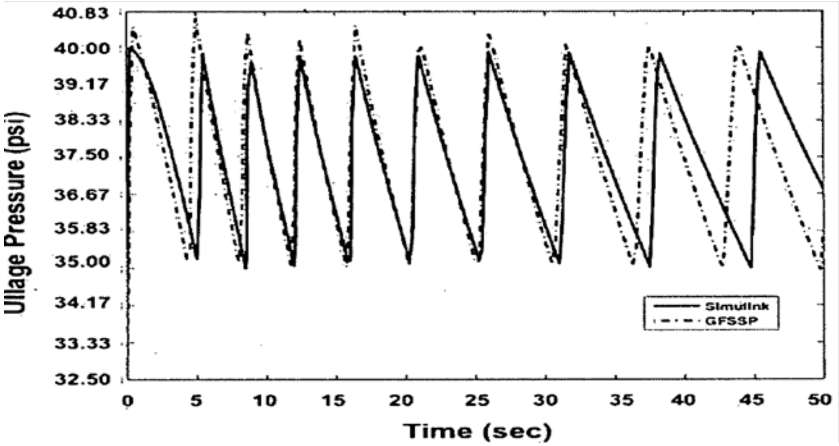

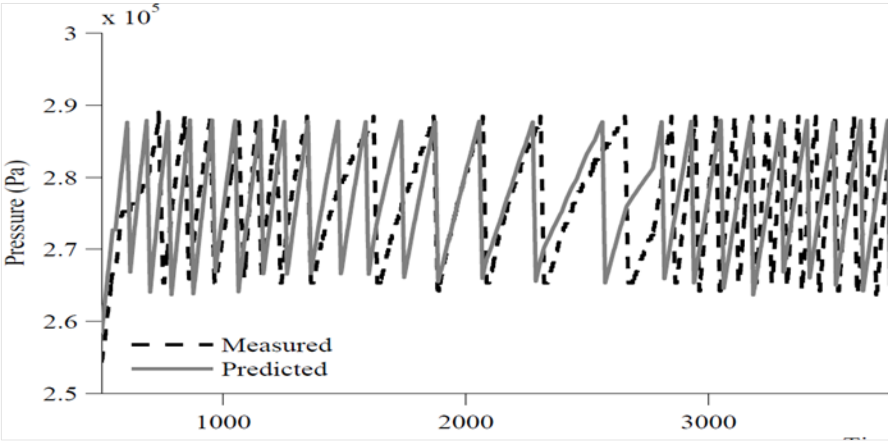

1. P.N. Estey, D. H. Lewis Jr.,t and M. Conno, “Prediction of a Propellant Tank Pressure History Using State Space Methods”, J. Spacecraft and Rockets, v. 20, (1983), p 49.
2. B.T. Burchett, “Simulink Model of the Ares I Upper Stage Main Propulsion System”, AIAA (2008)
3. V. V. Osipov et al, “A Dynamical Model of Rocket Propellant Loading with Liquid Hydrogen”, AIAA Journal of Spacecraft and Rockets, 2011

SINDA/FLUINT Tank model

Stratification (Continued) – GOES IV&V Pitch

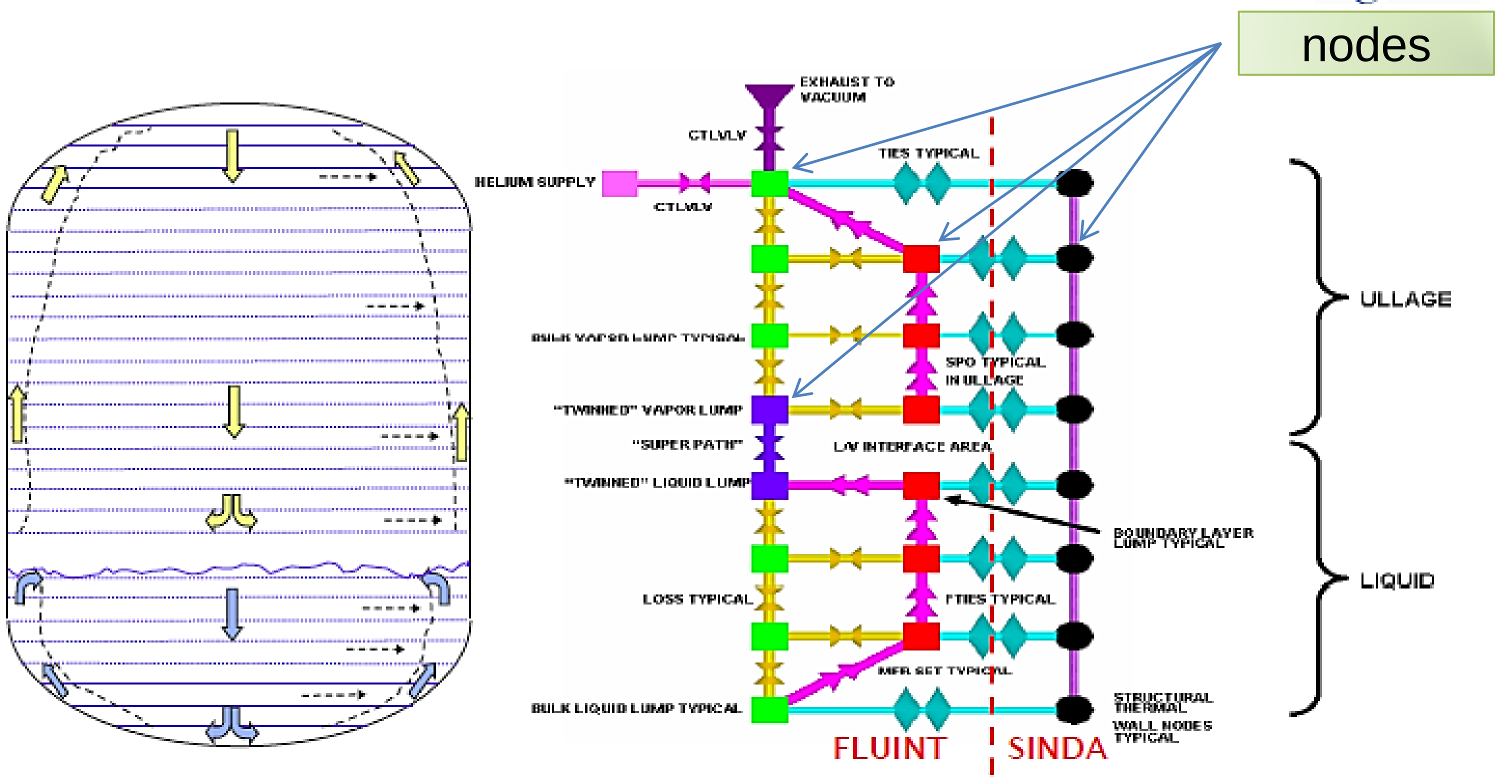

Schematic of modeling elements

Paul Schallhorn, "LSP Upper Stage Propellant Tank Thermodynamic Modeling", 2010

Model of the Chilldown and Propellant Loading of the Space Shuttle External Tank

The Generalized Fluid System Simulation Program (GFSSP)

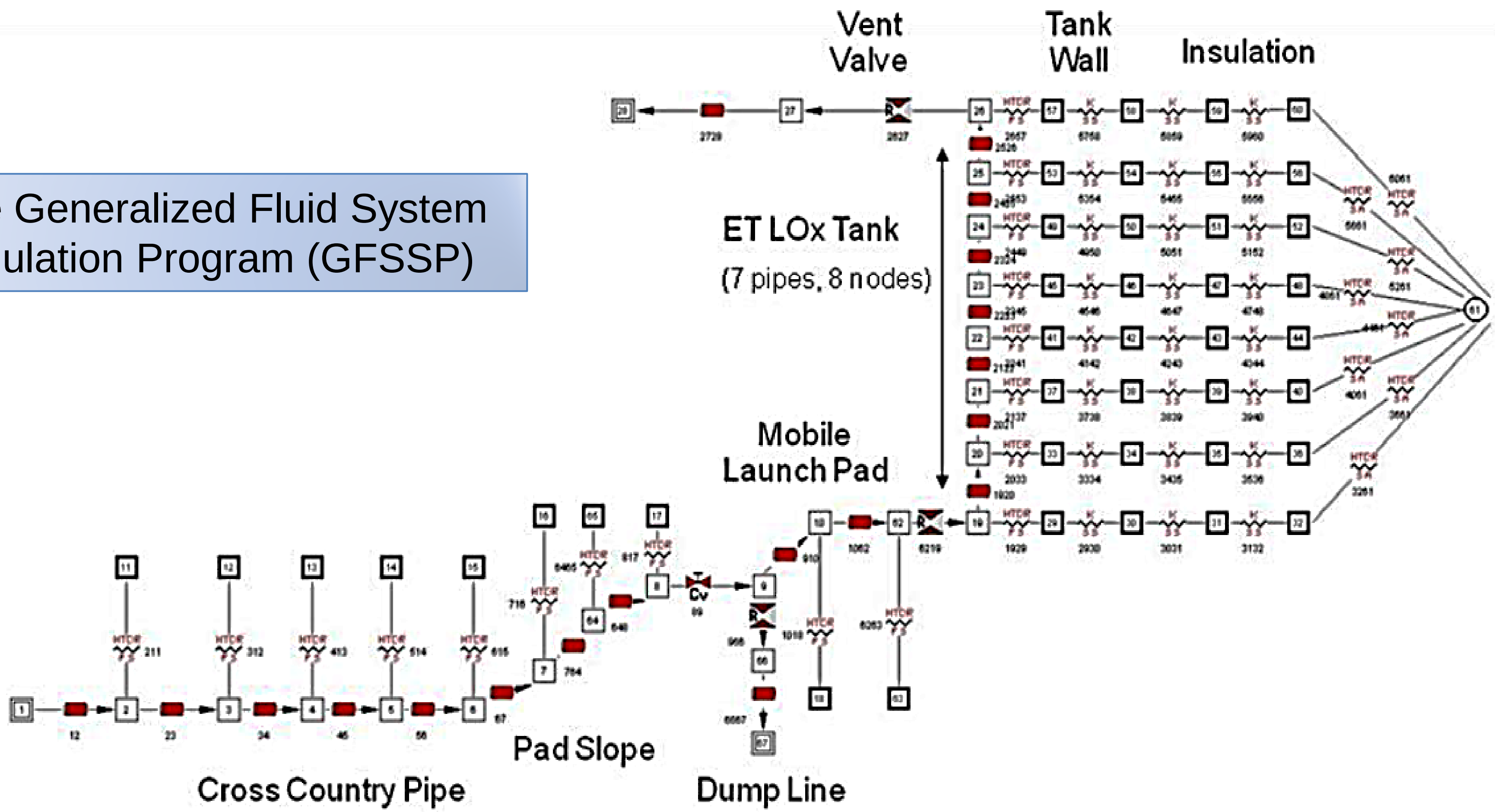

Figure 2. GFSSP Model of the KSC Ground System and Shuttle LOx Tank

A. C. LeClair and A. K. Majumdar, *NASA/Marshall Space Flight Center,* “Computational Model of the Chilldown and Propellant Loading of the Space Shuttle External Tank”, AIAA

GFSSP predictions

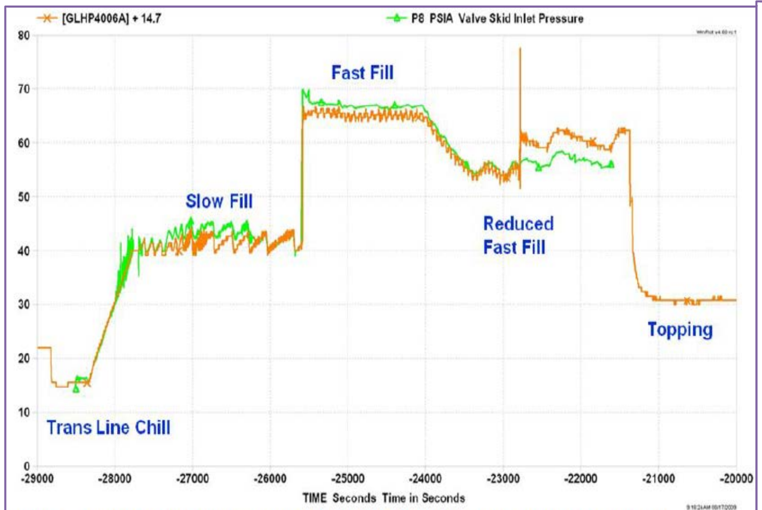

Figure 7. Measured and Predicted Pressure at the Inlet to the Fill Control Valve (psia)

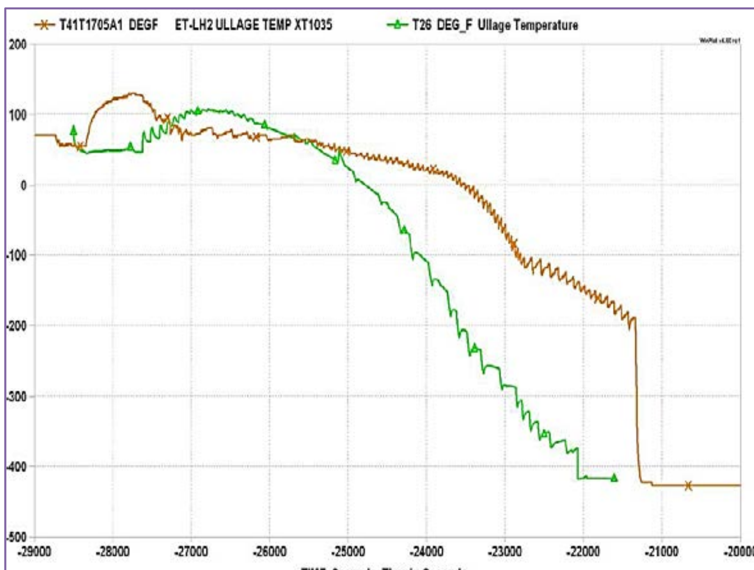

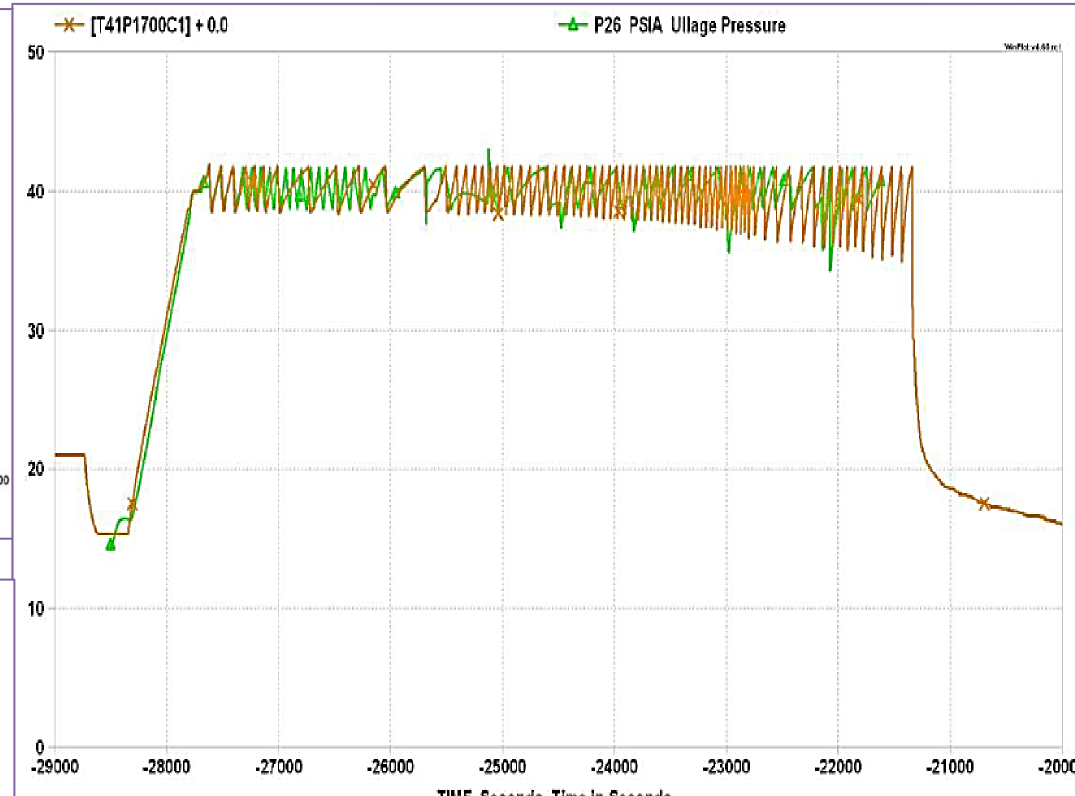

Measured and predicted ullage pressure in the LH2 tank. Agreement is excellent until slow fill begins, at which point the model is no longer able to match the pressure cycling that occurs during loading. This may be caused by the two phase mixture present in the tank once slow fill begins.

A. C. LeClair and A. K. Majumdar, “Computational Model of the Chilldown and Propellant Loading of the Space Shuttle External Tank”, AIAA

Problem Formulation

The future autonomous system capable of accomplishing launch vehicle propellant load and drain without human interaction should be able to change its behavior in response to un-anticipated events.

The complexity of this problem dictates the necessity of

- development of a physics based model for loading operation that can reproduce accurately the time traces during the loading,
- predict system response to various deviations from the loading protocol,
- detect and localize system faults online.

Methodology

- The main element of the model is the NODE. In general it contains 3D conservation equations for the mass, momentum, and the energy

$$\rho_{,t} + (\rho u_\alpha)_{,\alpha} = 0$$
$$(\rho u_\alpha)_{,t} + \left(\rho u_\alpha u_\beta\right)_{,\beta} = -p_{,\alpha} + \tau_{\alpha\beta,\beta}$$
$$(\rho E)_{,t} + (\rho E u_\alpha)_{,\alpha} = -(p u_\alpha)_{,\alpha} + \left(u_\alpha \tau_{\alpha\beta}\right)_{,\beta} + \left(\kappa T_{,\alpha}\right)_{,\alpha}$$

- In medium fidelity models the following assumptions are introduced
  - Dynamics is one-dimensional (or quasi-two dimensional)
  - Momentum equation is reduced $\nabla p=0$ (in low Mach approximation M << 1). Except for the pipe and valve losses
  - Equation of states of an ideal gas $E = c_v T; \quad p = \rho R T; \quad \rho E = p\, c_v / R = p / (\gamma - 1)$

$$\dot{m}^{(i)} = J_{in}^{(i)} - J_{out}^{(i)}$$
$$\dot{p} = -\frac{\gamma p}{V}\dot{V} + \frac{\gamma - 1}{V}\sum_{k=1}^{N}\dot{Q}_k$$
$$T = \frac{pV}{\sum_{i=1}^{N} m^{(i)} R^{(i)}}$$

Common types of the nodes

Ideal gas

$$\dot{m}^{(i)} = J_{in}^{(i)} - J_{out}^{(i)}$$

$$\dot{p} = -\frac{\gamma p}{V}\dot{V} + \frac{\gamma - 1}{V}\sum_{k=1}^{N}\dot{Q}_k$$

$$T = \frac{pV}{\sum_{i=1}^{N} m^{(i)} R^{(i)}}$$

BL node

Correlations for the natural and forced convection

Interface

$$\dot{Q}_l - \dot{Q}_v = J_{lv} h_{lv} + J_{lv} c_p \left(T_u - T_s\right)\left(\dot{Q}_l > \dot{Q}_v\right)$$

$$\rho_{,t} + (\rho u_\alpha)_{,\alpha} = 0$$

$$(\rho u_\alpha)_{,t} + \left(\rho u_\alpha u_\beta\right)_{,\beta} = -p_{,\alpha} + \tau_{\alpha\beta,\beta}$$

$$(\rho E)_{,t} + (\rho E u_\alpha)_{,\alpha} = -(p u_\alpha)_{,\alpha} + \left(u_\alpha \tau_{\alpha\beta}\right)_{,\beta} + \left(\kappa T_{,\alpha}\right)_{,\alpha}$$

Wall

$$\rho_w c_w V_w \, \partial T_w / \partial t = S_w h (T - T_w)$$

Liquid

$$\dot{m}^{(i)} = J_{in}^{(i)} - J_{out}^{(i)}$$

$$T = \text{const (20K or 77K)}$$

Pipe

$$f = \begin{cases} fL & Rey \le 2000 \\ fT & 4000 \le Rey \\ fL + \dfrac{(fT - fL)(Rey - ReL)}{ReT - ReL} & otherwise \end{cases}$$

Launchpad Sketch

Notice elevation at the Launchpad h=25.8m corresponding to ≈ 18 kPa

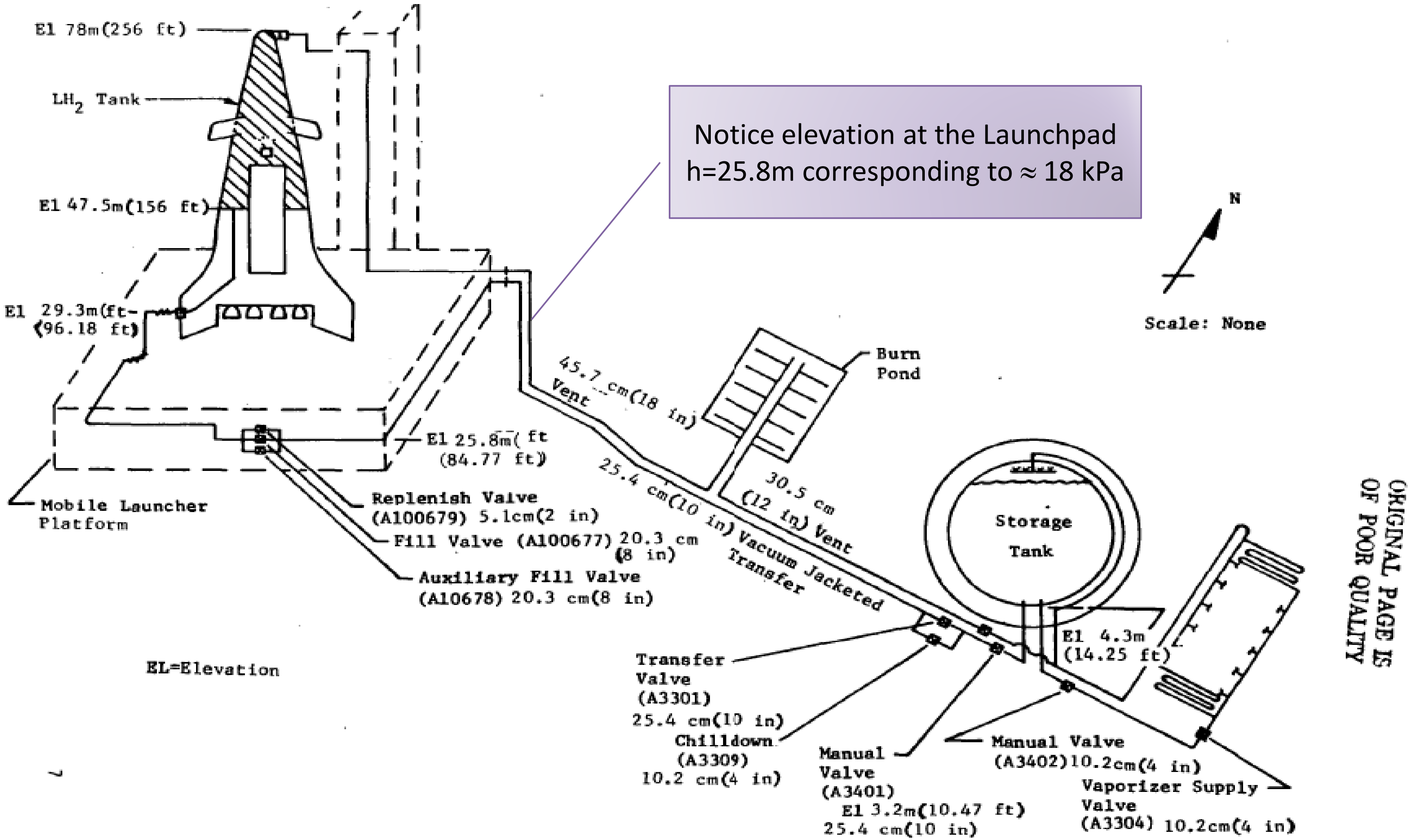

FIGURE II-2 KSC LC 39 SSTO/DENSIFIED HYDROGEN BASELINE LOADING SYSTEM

Node Presentation of our Original Model

1. The reduced model is described by **16 state time-dependent variables**

- LH2 , GH2 masses m_{l1}, m_{v1} in Storage Tank (ST, $i = 1$) – ***2 var***
- LH2 , GH2 and GHE m_{l2}, m_{v2}, m_{g2} masses in External Tank (ET, $i = 2$) – ***3 var***
- Pressure p_{v1} of GH2 in ST – ***1 var***
- Partial pressures p_{v2}, p_{g2} of GH2 and GHE in ET – ***2 var***
- Vapor/gas volumes V_{vi} in ST and ET – ***2 var***
- Vapor/gas temperatures T_{vi} in ST and ET – ***2 var***
- Liquid temperatures T_{li} in ST and ET – ***2 var***
- Film (surface) temperatures T_{fi} in ST and ET – ***2 var***

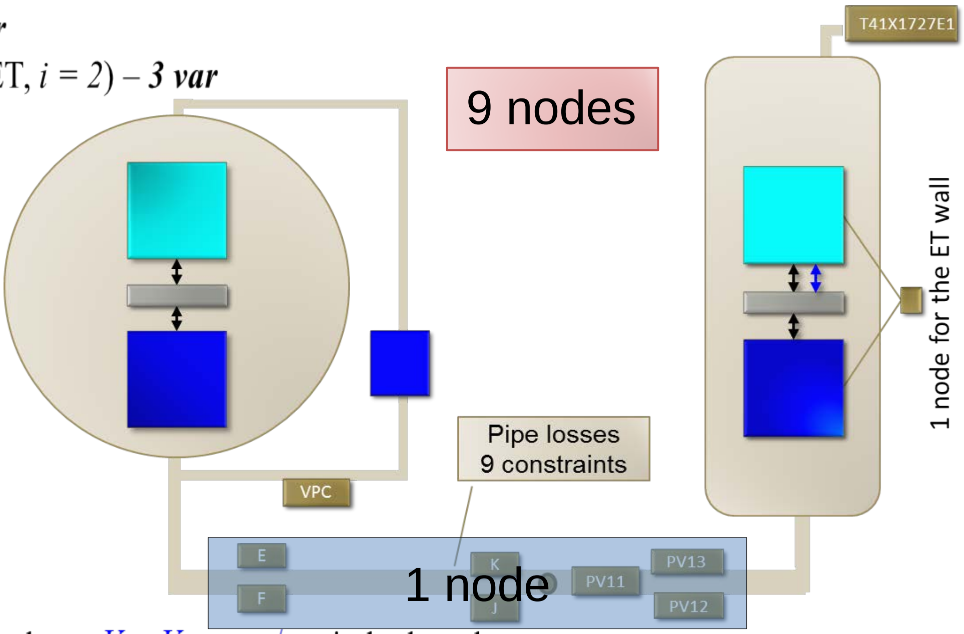

2. There are total **7 constraints** on state variables

- **2** Equations of state for GH2 in ST and ET: $p_{vi}V_{vi} = m_{vi}R_vT_{vi}$
- **1** Equations of state for GHE in ST: $p_{g2}V_{v2} = m_{g2}R_2T_{v2}$
- **2** Equations relating vapor/gas volume to LH2 mass and total volume $V_i = V_{vi} + m_{vi}/\rho_l$ in both tanks
- **2** Equations of state for film in both tanks: $p_{fi}\left(T_{fi}\right) = p_{vi} = p_C\left(T_f/T_C\right)^n$

3. There are total **9 ordinary time-dependent differential rate (and integral-differential) equations** for 16 – 7 = **9 independent variables**:

- 5 mass conservation equations (for LH2 and GH2 in both tanks and GHE in ET)
- 4 energy conservation equations (for GH2 and LH2 in both tanks)

9 Integral-Differential Equations

1) 5 Mass Conservation Rate Eqs:

ST tank

- LH2: $\dot{m}_{l1} = J_{lv1} - J_{boil} - J_{tr}$
- GH2: $\dot{m}_{v1} = J_{boil} - J_{v,vent1} - J_{lv1}$

ET tank

- LH2: $\dot{m}_{l2} = J_{lv2} + J_{tr}$
- GH2: $\dot{m}_{v2} = -J_{v,vent2} - J_{lv2}$
- GHE: $\dot{m}_{g2} = J_{g,in} - J_{g,vent2}$

Condensation-evaporation flow

J_{lvi} for $i = 1,2$ is determined by film energy conservation in ET and ST (see next slide)

Auxiliary rate equations:

Pressurizing mass flow from vaporizer:

$$\dot{J}_{boil} = \begin{cases} \left(J_{vap} - J_{boil}\right)/\tau_{vap}, & J_{vap} - J_{boil} \geq 0 \\ 0, & otherwise \end{cases}$$

Transfer line flow from ST to ET:

$$\dot{J}_{tr} = \left(\alpha_{eff}(t)\sqrt{|p_1 - p_2|} - J_{tr}\right)/\tau_{tr}$$

$J_{vap}(p_1, t), \alpha_{eff}(t)$

$J_{v,vent\,i}(p_i, t)$

$J_{g,vent\,2}(p_2, t), J_{g,in}(p_2, t)$

are all determined by filling protocol

Comparison with Real Data: ET

Theoretical prediction for valve on-off oscillation loses its phase relative to experimental oscillations due to transient boil-off events in the ET, but once the transient decays, the phase of oscillation is recovered and the theoretical model correctly predicts real data.

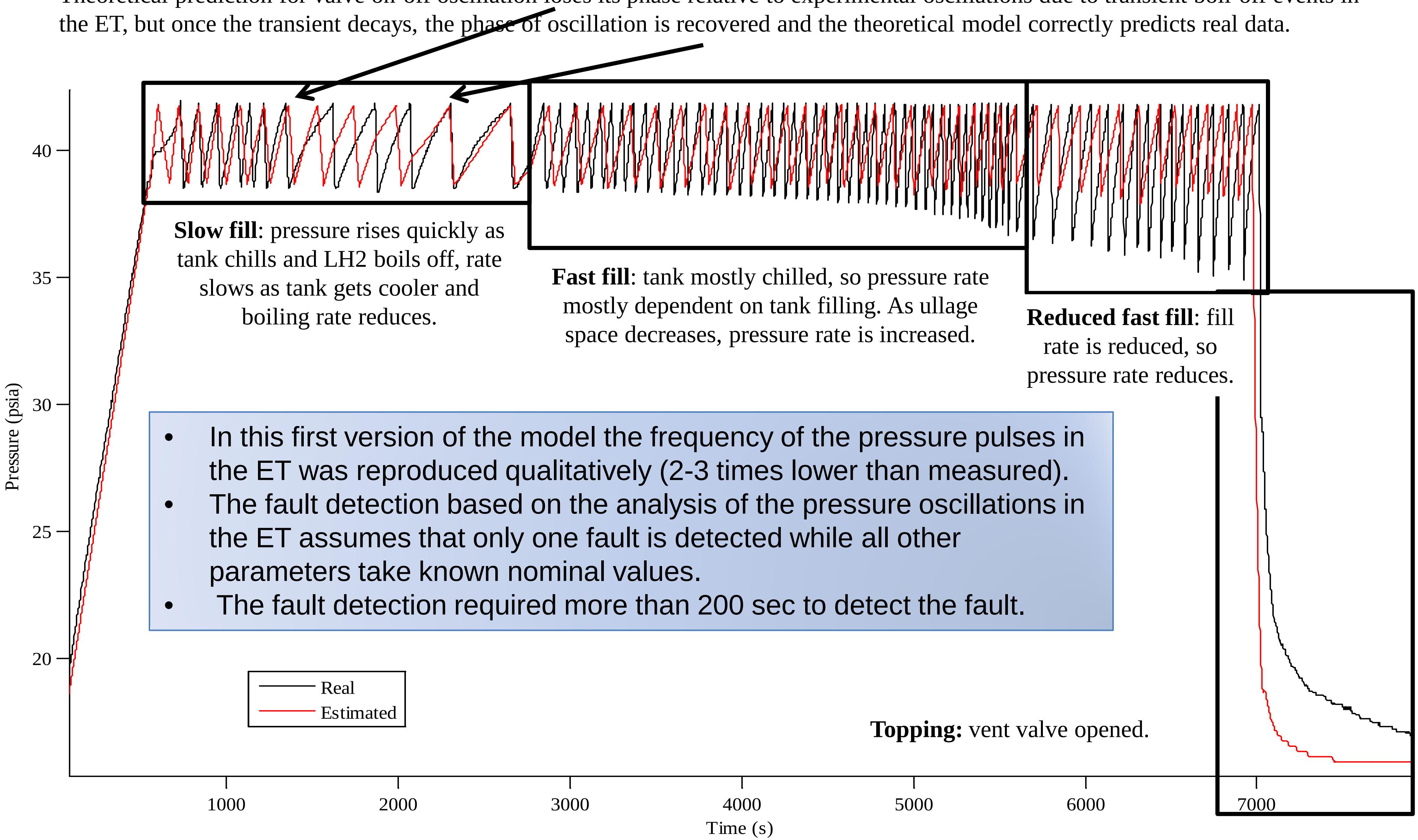

- In this first version of the model the frequency of the pressure pulses in the ET was reproduced qualitatively (2-3 times lower than measured).
- The fault detection based on the analysis of the pressure oscillations in the ET assumes that only one fault is detected while all other parameters take known nominal values.
- The fault detection required more than 200 sec to detect the fault.

Model of LH2 Loading

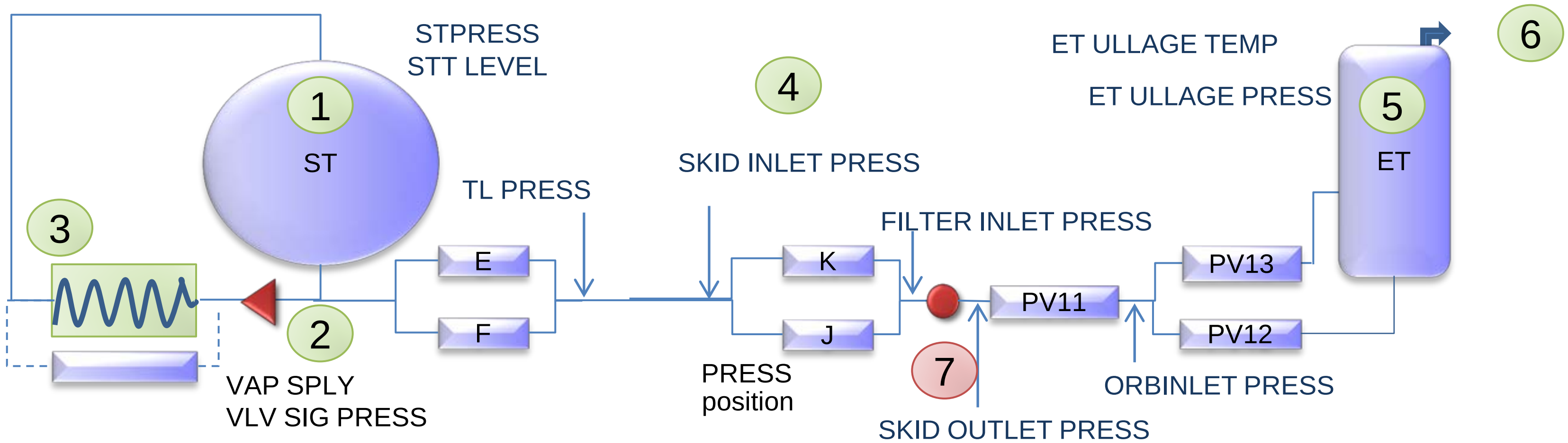

	E	F	J	K	PV11	PV12	PV13	
Pressurization (GH2)	0	0	0	1	1	1	0	Pressurization (GHe)
Slow Fill: 553-2773s	0	1	0	1	1	1	1	1000
Fast Fill: 2773-5570s	1	1	0	1	1	1	1	7500 gpm
Reduced: 5570-6988s	1	1	1	0.1	1	1	1	850 gpm
Topping: 6988-9630s	0	1	1	0.1	1	0	1	800 gpm
Replenish: to EOR	0	1	Ctrl	0	1	0	1	mass preserving

How many nodes should we add?

- In general IDAE model can be written in the form $F_i\left(t,\dot{\vec{x}},\vec{x},\vec{a},\vec{u}\right)=0$
- The output of the model is a set of time series data $\left\{x_i\left(t,\vec{a},\vec{u}\right)\right\}$
- That have to be compared with experimental data $\left\{y_i\left(t,\vec{a},\vec{u}\right)\right\}$

FD&I

Optimization

Validation

$$L=\sum_{i,j}\left(x_i\left(t_m\right)-y_i\left(t_m\right)\right)^2$$

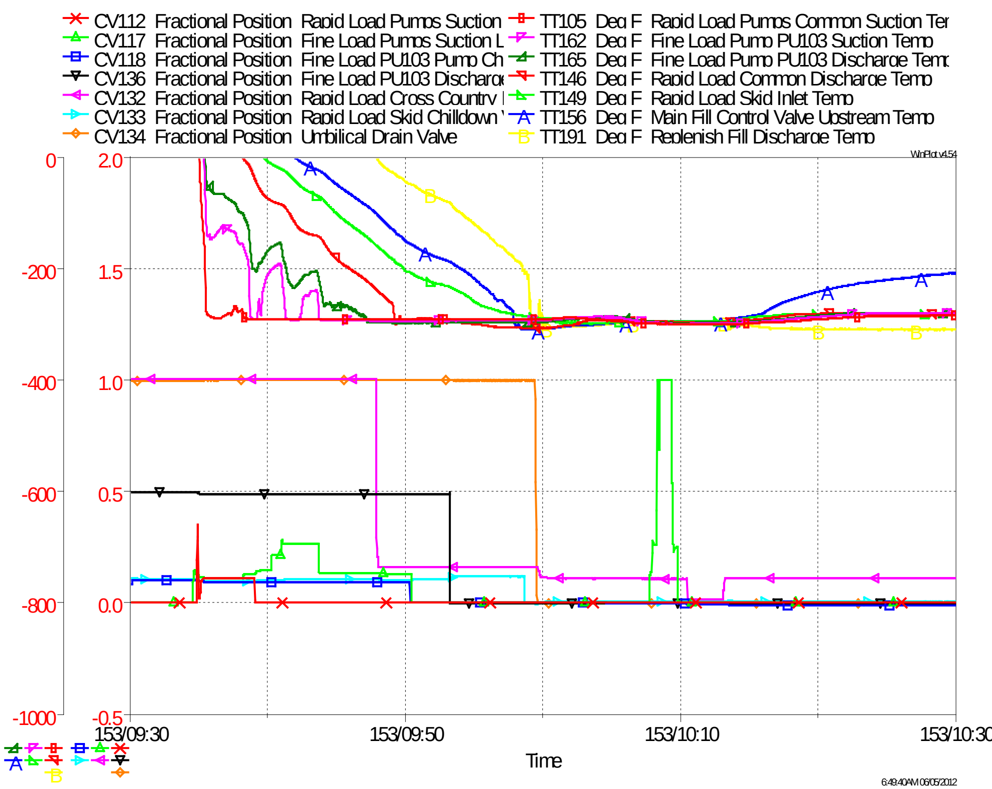

In a sense that the loss function is minimized and takes values below of some given threshold determined by the required accuracy of predictions.

We need minimum number of nodes that satisfy this criteria.

1 Storage Tank Equations

ID

$$\dot{m}_v = -J_{cd} + J_{vap,in}$$

$$\dot{p}_u = -\frac{\gamma p_u}{V_u}\dot{V}_u + \frac{\gamma - 1}{V_u}\left(J_{vap,in}h_{vap,in} - \dot{Q}_{wv} - \dot{Q}_v - J_{cd}c_p T_f\right)$$

$$T_u = p_u V_u / m_v R_v$$

Wall

$$\dot{T}_{w,i} = h_{w,i}\left(T_u - T_{w,i}\right) / \rho_w l_w c_w$$

Tank wall

Lq

$$\dot{m}_l = J_{cd} - J_{tr} - J_{vap,out}$$

$$T_l = 20K$$

Int

$$\dot{Q}_v - \dot{Q}_l + J_{cd}h_{cd} = 0; \quad T_f = f\left(p_{u,v}\right)$$

$$p_v V_u = m_v R_v T_u \qquad p_g V_u = m_g R_g T_u \qquad \left(p_v + p_g\right)V_u = \left(m_v R_v + m_g R_g\right)T_u$$

Lq

$$\dot{m}_{vap} = J_{vap}^{out} - J_{vap}^{in}$$

$$J_{vap}^{out} = S_{vap}\lambda_{vap}\rho_l\sqrt{g\left(L_l + L_{ST}\right)}$$

$$J_{vap}^{in} = \frac{0.62 \cdot m_{vap}\left[2p_u / R\left(T_{vap,w} + T_f\right)\right]^{1/4}}{\rho_l \pi R_w^2\left(h_{ev} + 0.5c_p\left(T_{vap,w} - T_f\right)\right)}\left[\frac{\kappa_g^3 \rho_f g h_{cd}}{\mu_g\left(T_w - T_f\right)D}\right]^{1/4}$$

Vaporizer

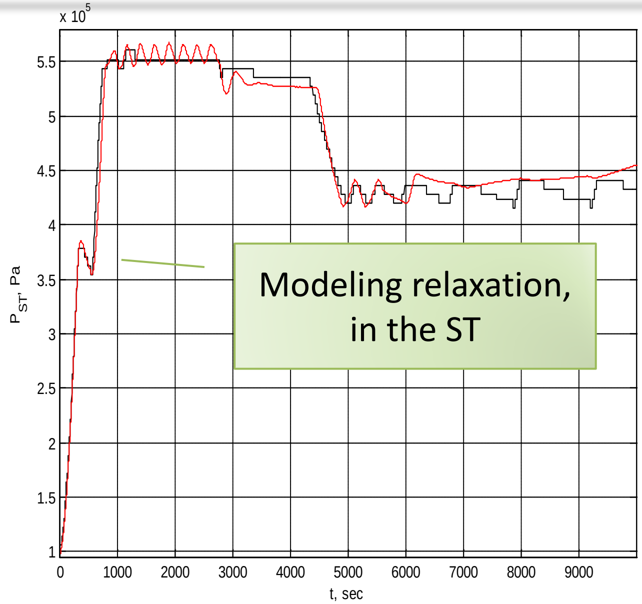

Modeling relaxation, in the ST

3 Vaporizer Equations

$$\dot{m}_{l,vap} = J_{vap}^{in} - J_{vap}^{out}$$

$$J_{vap}^{in} = S_{vap}\lambda_{vap}\rho_l\sqrt{g\left(L_l + L_{ST}\right)}$$

This is valve equation $J_{vap} = \alpha_{vap}\sqrt{\Delta P}$

$$J_{vap}^{out} = S_{vap,w}\cdot q_{vap}\Big/\left(h_{ev} + 0.5c_p\left(T_{vap,w} - T_l\right)\right)$$

Wall film boiling correlations [1]

$$q_{vap} = Nu_D\cdot\kappa / D \approx 0.62\left[\frac{\kappa_g^3\rho_g\rho_l g h_{cd}}{\mu_g\left(T_w - T_{sat}\right)D}\right]^{1/4}$$

$$S_{vap,w} = 2\pi R_w L_{vap,w} = 2m_{l,vap} / \rho_l R_w$$

$$\rho_g = 2p_u / R\left(T_{vap,w} + T_{sat}\right)$$

$$L_{vap,w} = \frac{V_{vap}}{\pi R_w^2} = \frac{m_{vap}}{\rho_l\pi R_w^2}$$

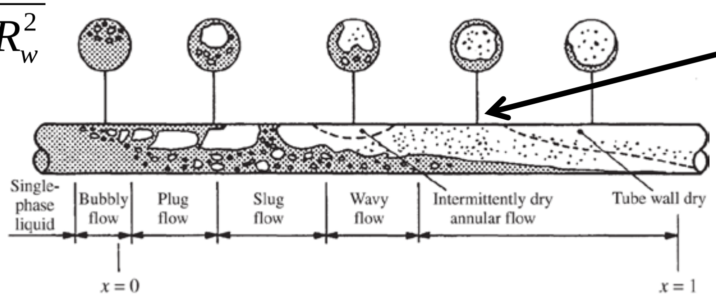

[1] J.H.Lienhard and J.H.Lienhard, “A heat transfer textbook”, 3rd ed., Cambridge, Phlogiston Press, 2003

2 Vaporizer Pressure Control

$$\dot{S}_{vap} = \left(S_{vap,0} - S_{vap}\right)/\tau$$

$$S_{vap,0} = S_{vap,stab} - A_{vap} \cdot \left(P_{ST} - P_{ST,fast}\right) / P_{ST,fast}$$

In stabilization regime

$$\lambda_{vap} = \left(S_{vap} > 1.015 S_{vap,stab}\right)\left(1\text{-}\lambda_{vap}\right) + \left(S_{vap} > 0.985 S_{vap,stab}\right)\lambda_{vap}$$

1. Open to pressurize up to 3.75 x 10^5 Pa
2. Wait for ET to complete pressurization
3. Open to pressurize up to 76.5 x 10^5 Pa
4. Stabilize at the level 80.7 x 10^5 Pa

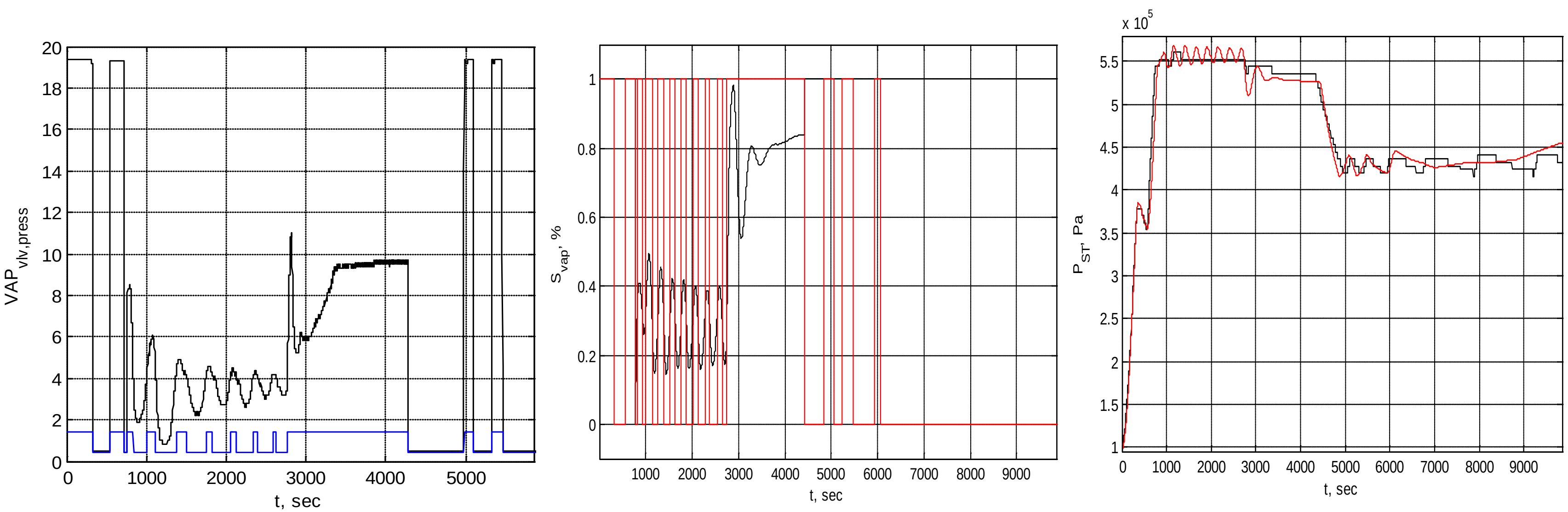

5 ET Equations

Added wall nodes and correct geometry of the ET

ID

$$\dot{m}_v = -J_{cd} - J_{vent,v} + J_b$$

$$\dot{m}_g = J_{g,in} - J_{vent,g}$$

$$\dot{p}_u = -\frac{\gamma p_u}{V_u}\dot{V}_u + \frac{\gamma - 1}{V_u}\left(J_{g,in}h_{g,in} + J_b c_{p,v} T_b - J_{vent,v} c_{p,v} T_u - J_{vent,g} c_{p,g} T_u - \dot{Q}_{wv} - \dot{Q}_v - J_{cd} c_p T_f\right)$$

$$T_u = p_u V_u \big/ \left(m_v R_v + m_g R_{vg}\right)$$

Wall

$$\dot{T}_{w,i} = h_{w,i}\left(T_u - T_{w,i}\right) \big/ \rho_w l_w c_w$$

Lq

$$\dot{m}_l = J_{cd} + J_{tr} - J_b$$

$$T_l = 20K$$

Int

$$\dot{Q}_v - \dot{Q}_l + J_{cd} h_{cd} = 0$$

$$T_f = f\left(p_{u,v}\right)$$

$$\rho = \rho_v + \rho_g$$

Vnt

$$J_{vent,v(g)} = \lambda_{vvent} \cdot S_{valve} \cdot \rho_{v(g)} \sqrt{\gamma p_g / \rho \Gamma^2},$$

$$p_v V_u = m_v R_v T_u \qquad p_g V_u = m_g R_g T_u \qquad \left(p_v + p_g\right) V_u = \left(m_v R_v + m_g R_g\right) T_u$$

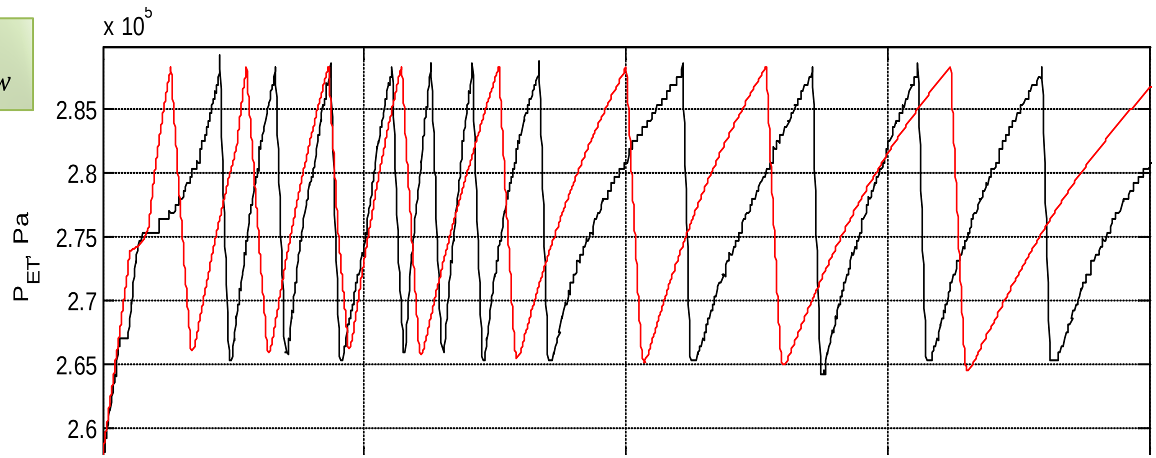

6 ET Vent valve dynamics

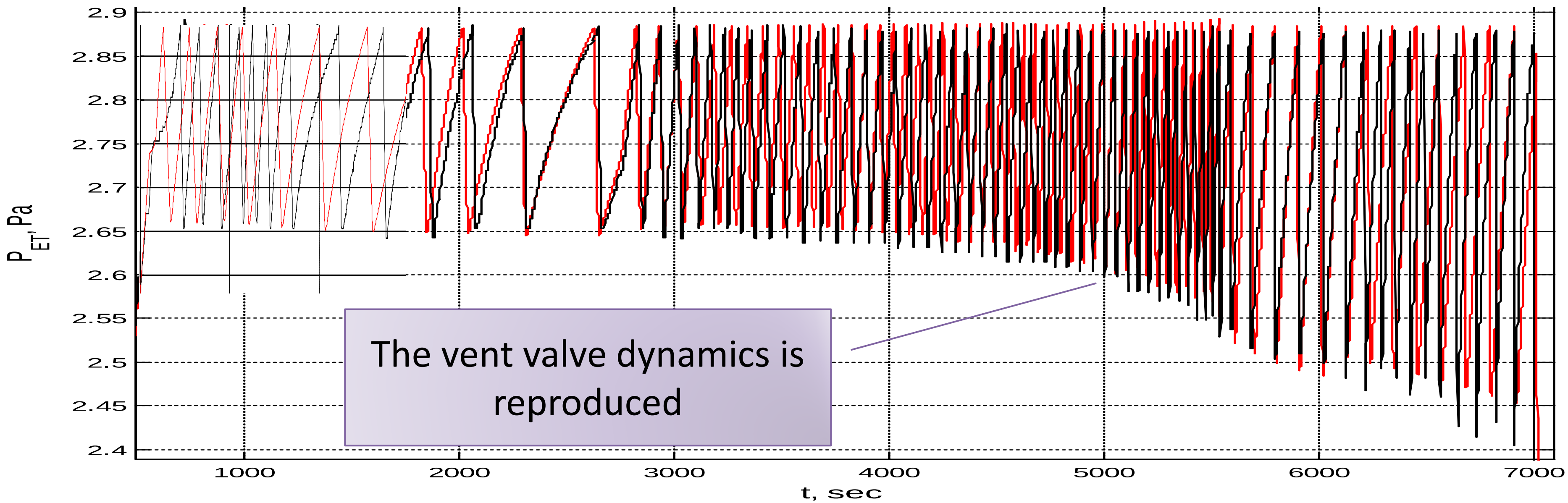

$$\lambda_{vent0} = \left(p_{ET} \geq p_{ET,high} \right) + \left(p_{ET,low} < p_{ET} < p_{ET,high} \right) \cdot \lambda_{vent0}$$

$$\dot{\lambda}_{vent} = \frac{\lambda_{vent0} - \lambda_{vent}}{\tau_{vent}}$$

$$J_{vent,v(g)} = \lambda_{vent} \cdot S_{vent} \cdot \rho_{v(g)} \sqrt{\gamma p_g / \rho \Gamma^2},$$

$$\tau_{vent} = \begin{cases} \tau_{slow}, & \text{when open} \\ \tau_{fast}, & \text{when close} \end{cases}$$

4 Pipe Losses and Pipe Networks

Chezy Darcy's prediction $\Delta p = RQ^n$

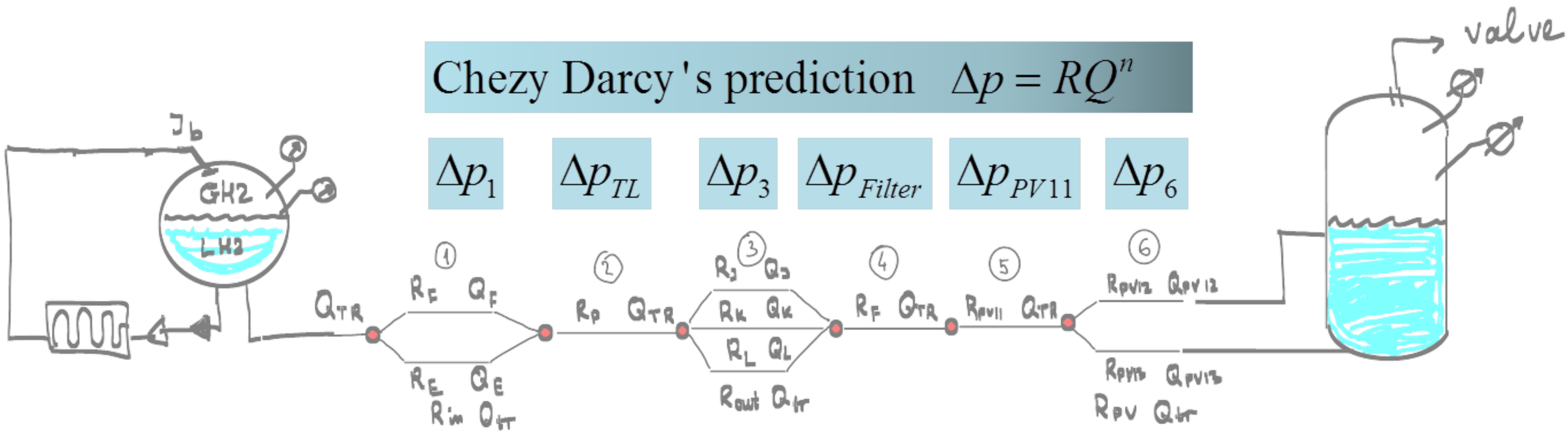

$$\Delta p = \sum_{i=1}^{N} \Delta p_i = \sum_{i=1}^{N} R_i Q^2 = Q^2 \sum_{i=1}^{N} R_i$$

	E	F	J	K	PV11	PV12	PV13
Press	0	0	0	1	1	1	0
Slow	0	1	0	1	1	1	1
Fast	1	1	0	1	1	1	1
Reduced	1	1	1	0.1	1	0	1
Topping	0	1	1	0.1	1	0	1
Replenish	0	1	Ctrl	0	1	0	1

Example. Resistance of the skid valves

$$R_3 = \left(\lambda_K R_K^{-\frac{1}{2}} + \lambda_L R_J^{-\frac{1}{2}}\right)^{-2}$$

$$R_3^{(S,F)} = R_K$$

$$R_3^{-\frac{1}{2}} = 0.1(R_K)^{-\frac{1}{2}} + R_J^{-\frac{1}{2}}$$

$$R_K^F = \Delta p_K^F / Q^2$$

The differential pressure along the line

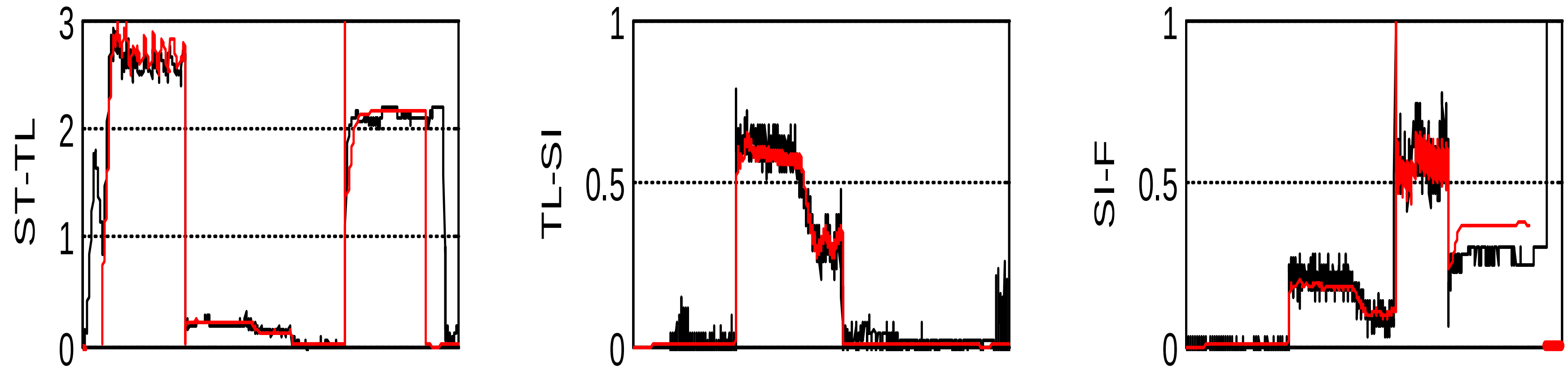

The model can reproduce quite accurately pressure changes along the line including losses at the control valves near the ST, at the skid, and orbiter inlet..

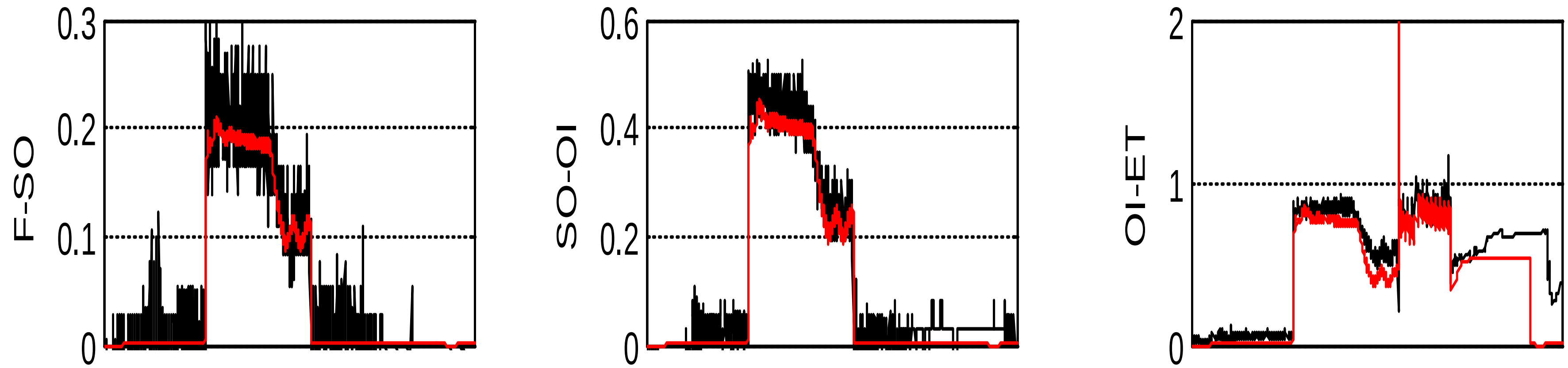

The measurements of the differential pressure signals provide a very sensitive tool for simultaneous fault detection along the line.

Additional Chilldown During Loading

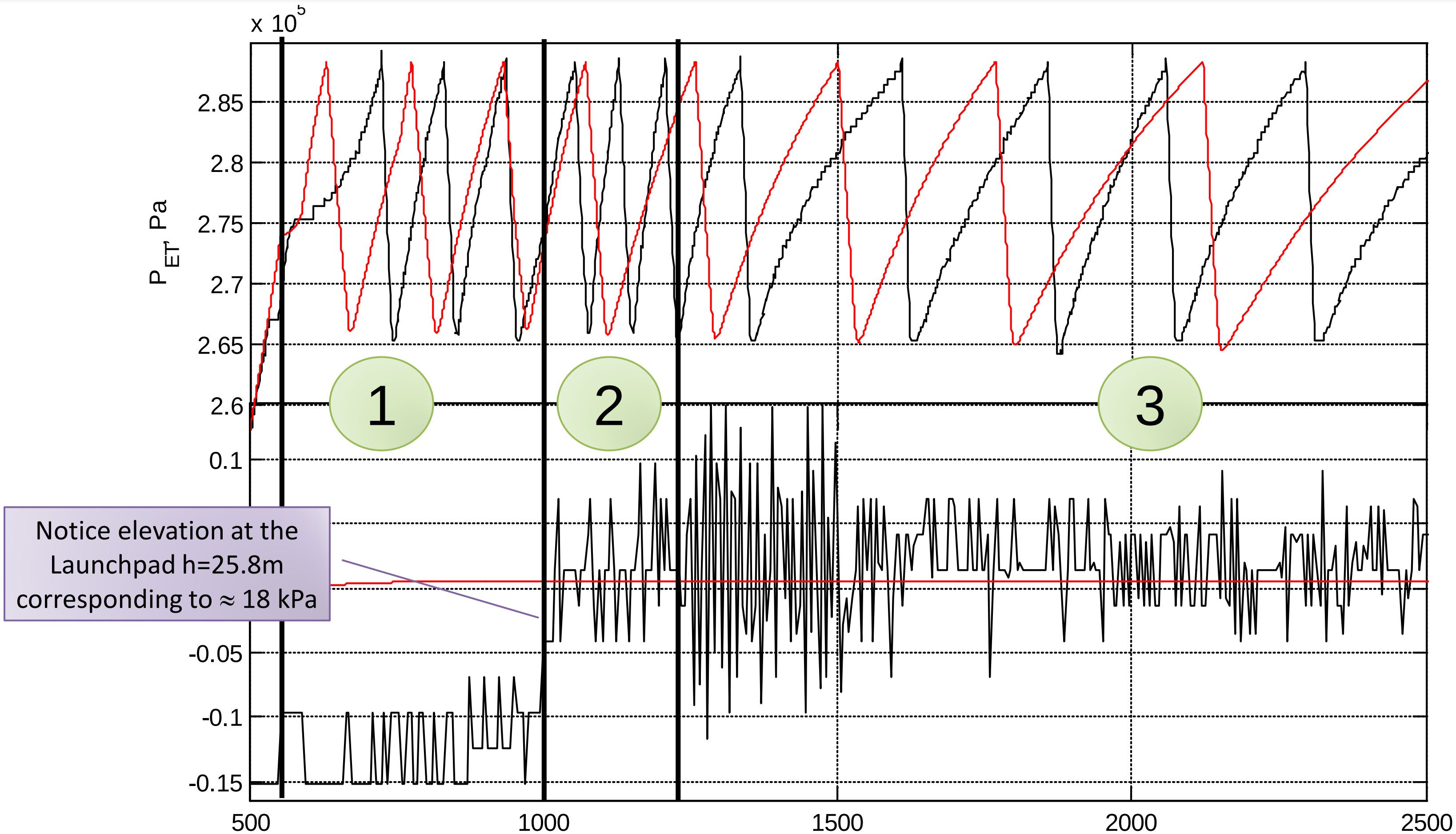

The analysis of the model predictions leads to the conclusion that the launch pad facility is not fill with the liquid until 1000 sec into the loading operation. This conclusion was later confirmed by the launch pad engineers demonstrating the consistency of the model.

4 + 5 Chilldown Model

Lq

$$\dot{m}_{p,l} = J_{tr} - J_{p,b}; \quad T_l = 20K$$

ID

$$\dot{m}_{p,v} = J_{p,b} - J_{p,out}$$

$$\dot{p}_p = -\frac{\gamma p_p}{V_p}\dot{V}_p + \frac{\gamma - 1}{V_p}\left(J_{pb} c_p T_{pb} - J_{p,out} c_p T_{p,ET} - \dot{Q}_{pw,v}\right)$$

Wall

$$\dot{T}_{pw,i} = h_{pw,i}^{(v,l)}\left(T_{(v,l)} - T_{pw,i}\right)\Big/\rho_{pw} l_{pw} c_{pw}$$

$$J_{pb,i} = h_{pw,i}^{(l)}\left(T_{(l)} - T_{pw,i}\right)/\left(h_{ev} + 0.5\left(T_{l,s} + T_{w,i}\right)\right)$$

ID

$$\dot{m}_v = -J_{vnt,v} + J_{p,out}$$

$$\dot{m}_g = J_{g,in} - J_{vnt,g}$$

$$\dot{p}_{ET} = \frac{\gamma - 1}{V_{ET}}\left(\dot{Q}_{he} + J_{p,out} c_p T_{p,ET} - \dot{Q}_{vnt,v} - \dot{Q}_{vnt,g} - \dot{Q}_{wv}\right)$$

$$T_{ET} = p_{ET} V_{ET}\Big/\left(m_v R_v + m_g R_{vg}\right)$$

Lq

$$\dot{m}_{ET,l} = J_{tr} + J_{cd} - J_b$$

Int

$$\dot{T}_{w,i} = h_{w,i}\left(T_{ET} - T_{w,i}\right)\Big/\rho_w l_w c_w$$

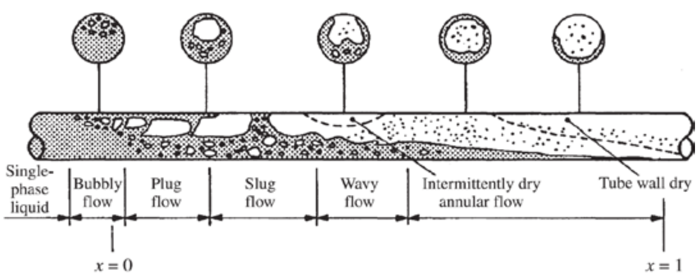

Forced convection correlation for horizontal pipes

- For the smooth tubes we use Petukhov correlation

$$f = \left(0.79 \cdot ln\left(Re_{D_h}\right) - 1.64\right)^{-2} \text{ for } 10^4 < Re < 10^6$$

- For fully developed flow. The Nusselt Number is given by the Petukhov correlation

$$Nu_{D_h,f} = \frac{(f/8)\left(Re_{D_h} - 1000\right)Pr}{1 + 12.7(Pr^{2/3} - 1)\sqrt{f/8}}$$

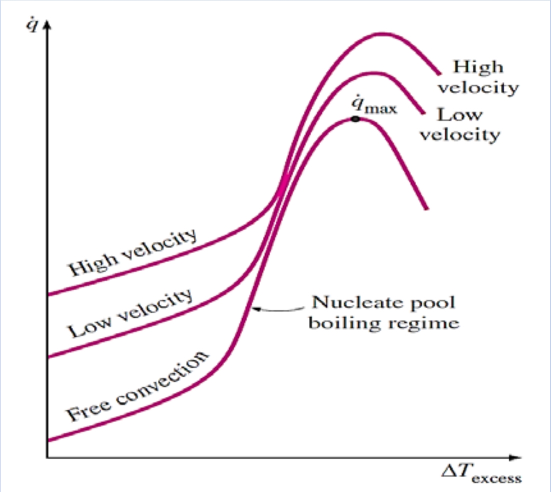

The effect of forced convection on external flow boiling for different flow velocities.

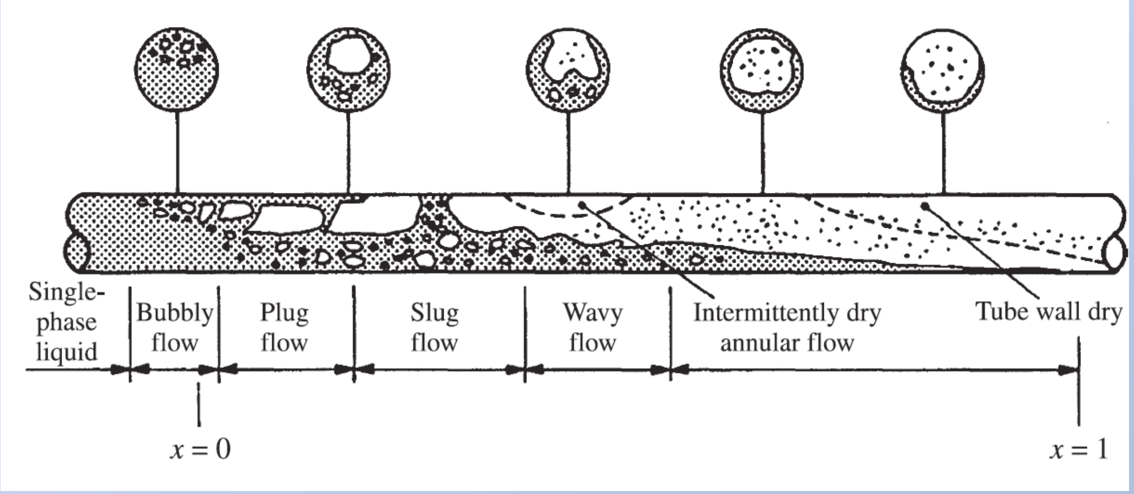

Flow patterns during evaporation in a horizontal tube with a uniform heat flux. (From Collier and Thome, 1994.)

G. NELLIS, S. KLEIN, “Heat Transfer”, Cambridge University Press

Flow boiling correlation for horizontal pipes

- The convection number *Co*: $$Co = \left(1/x - 1\right)^{0.8} \sqrt{\rho_{v,sat}/\rho_{l,sat}}$$
- The *Bo* is the boiling number, defined as the ratio of the heat flux at the wall to the heat flux required to completely vaporize the fluid $$Bo = h/Gh_{ev}$$
- The Froude number *Fr* is defined as the ratio of the inertial force of the fluid to the gravitational force $$Fr = G^2/\left(\rho_{l,sat}^2 g D_h\right)$$

according to Shah the Reynolds number should be evaluated using the liquid mass velocity, $G(1\text{-}x)$, while the Froude number should be evaluated using the total mass velocity, G.

$$N = \begin{cases} Co & \text{for vertical tubes or horizontal tubes with } Fr > 0.04 \\ 0.38\, Co\, Fr^{-0.3} & \text{for horizontal tubes with } Fr \le 0.04 \end{cases}$$

The Shah correlation is expressed by Eqs. (7-17) through (7-21):

$$\tilde{h}_{cb} = 1.8 N^{-0.8}$$

$$\tilde{h}_{nb} = \begin{cases} 230\sqrt{Bo} & \text{if } Bo \ge 0.3 \times 10^{-4} \\ 1 + 46\sqrt{Bo} & \text{if } Bo < 0.3 \times 10^{-4} \end{cases}$$

$$\tilde{h}_{bs,1} = \begin{cases} 14.70\sqrt{Bo}\, \exp(2.74 N^{-0.1}) & \text{if } Bo \ge 11 \times 10^{-4} \\ 15.43\sqrt{Bo}\, \exp(2.74 N^{-0.1}) & \text{if } Bo < 11 \times 10^{-4} \end{cases}$$

$$\tilde{h}_{bs,2} = \begin{cases} 14.70\sqrt{Bo}\, \exp(2.47 N^{-0.15}) & \text{if } Bo \ge 11 \times 10^{-4} \\ 15.43\sqrt{Bo}\, \exp(2.47 N^{-0.15}) & \text{if } Bo < 11 \times 10^{-4} \end{cases}$$

$$\tilde{h} = \begin{cases} \mathrm{MAX}(\tilde{h}_{cb}, \tilde{h}_{bs,2}) & \text{if } N \le 0.1 \\ \mathrm{MAX}(\tilde{h}_{cb}, \tilde{h}_{bs,1}) & \text{if } 0.1 < N \le 1.0 \\ \mathrm{MAX}(\tilde{h}_{cb}, \tilde{h}_{nb}) & \text{if } N > 0.1 \end{cases}$$

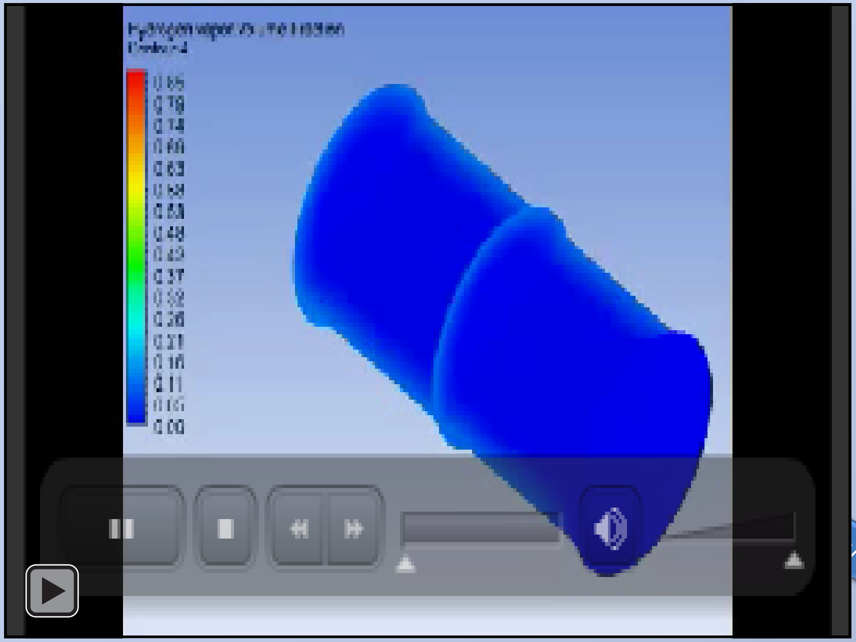

Modeling Chilldown

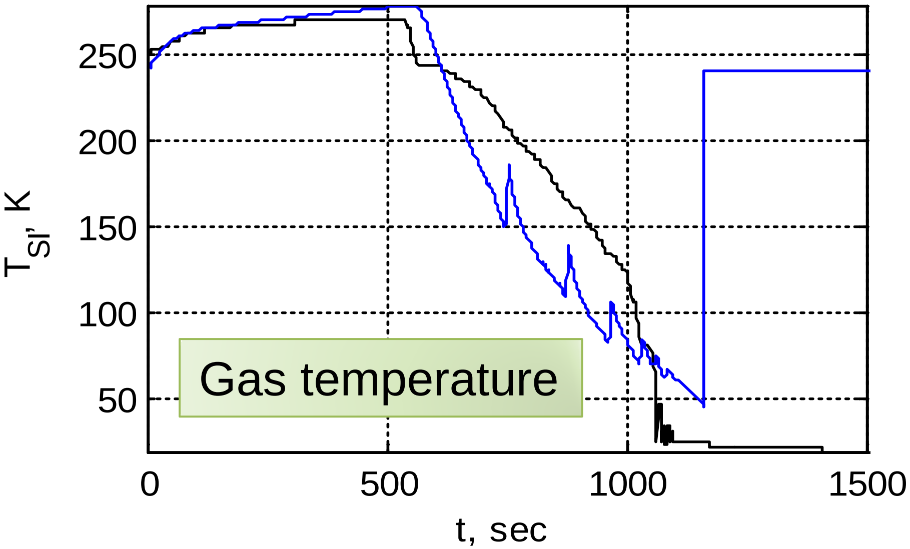

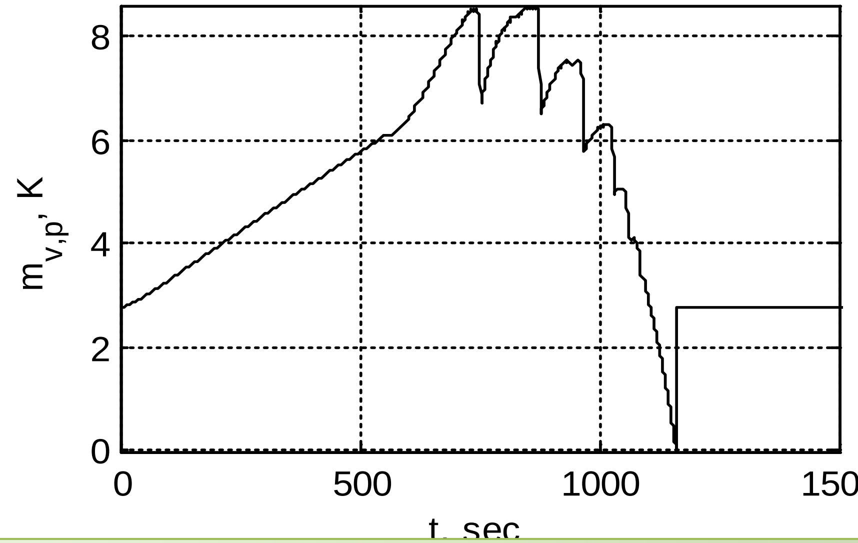

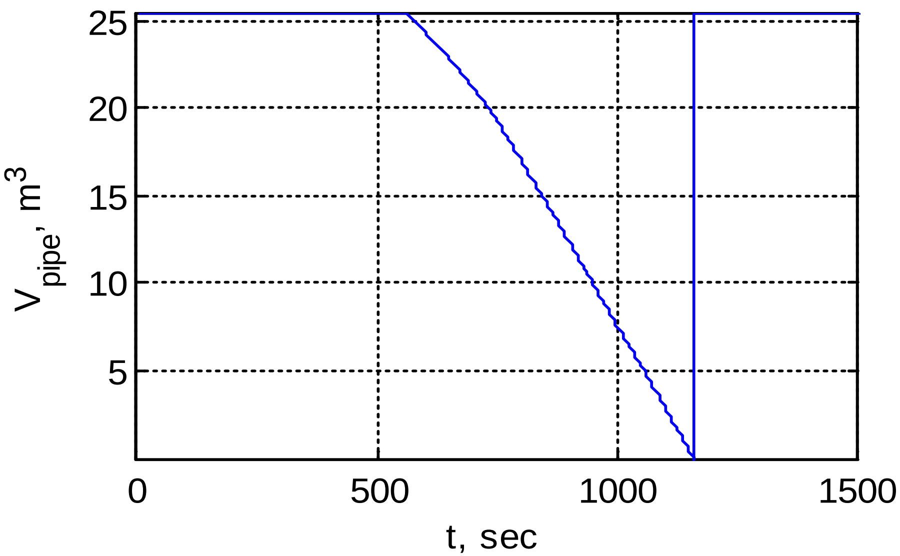

Wall temperature at different instance of time

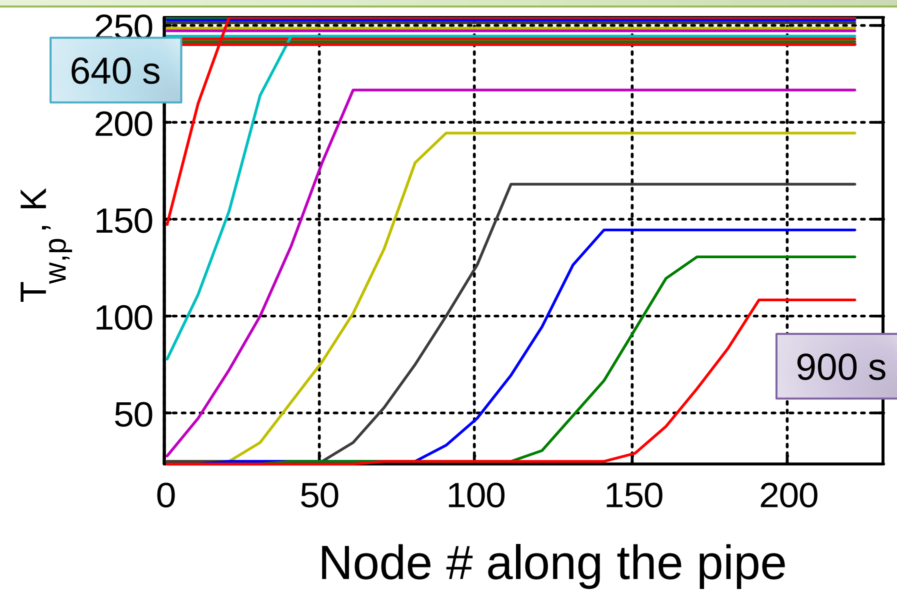

New Capabilities and Sensitivity

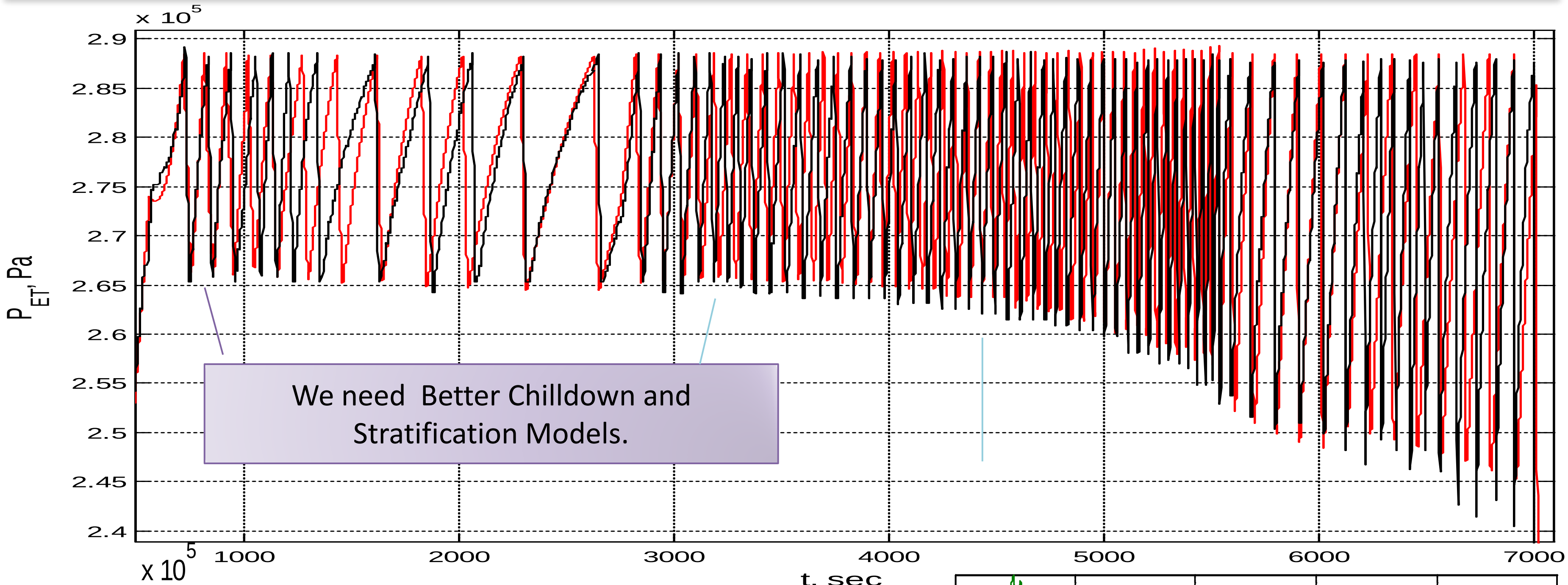

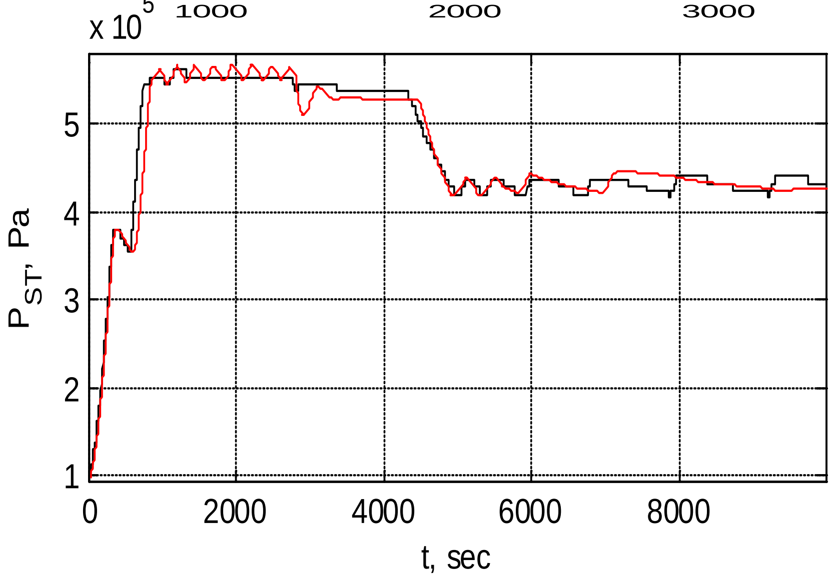

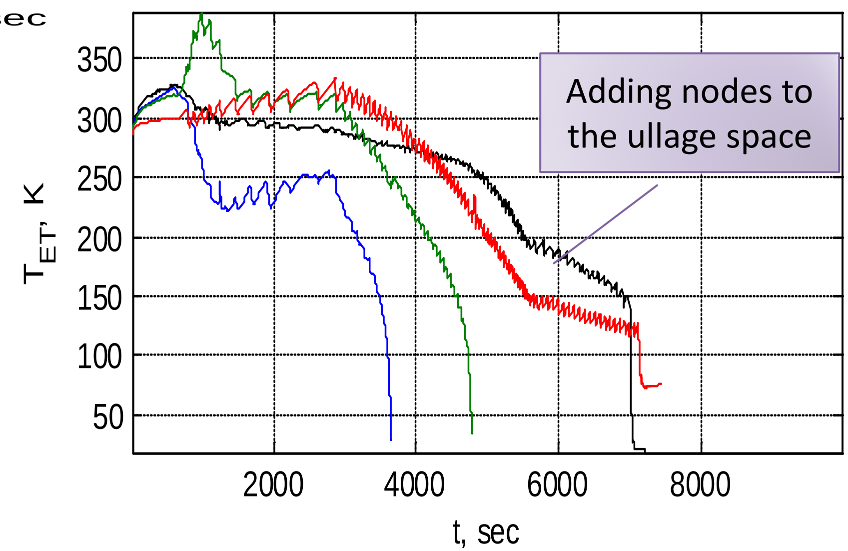

Fault Detection and Isolation

We now demonstrate that the developed model can be used to detect and isolate multiple faults including

- Blocking of the pressures control valve of the vaporizer
- Clogging of the valves along the transfer line
- Heat and mass leaks in the vehicle tank

Capabilities: pressure control fault

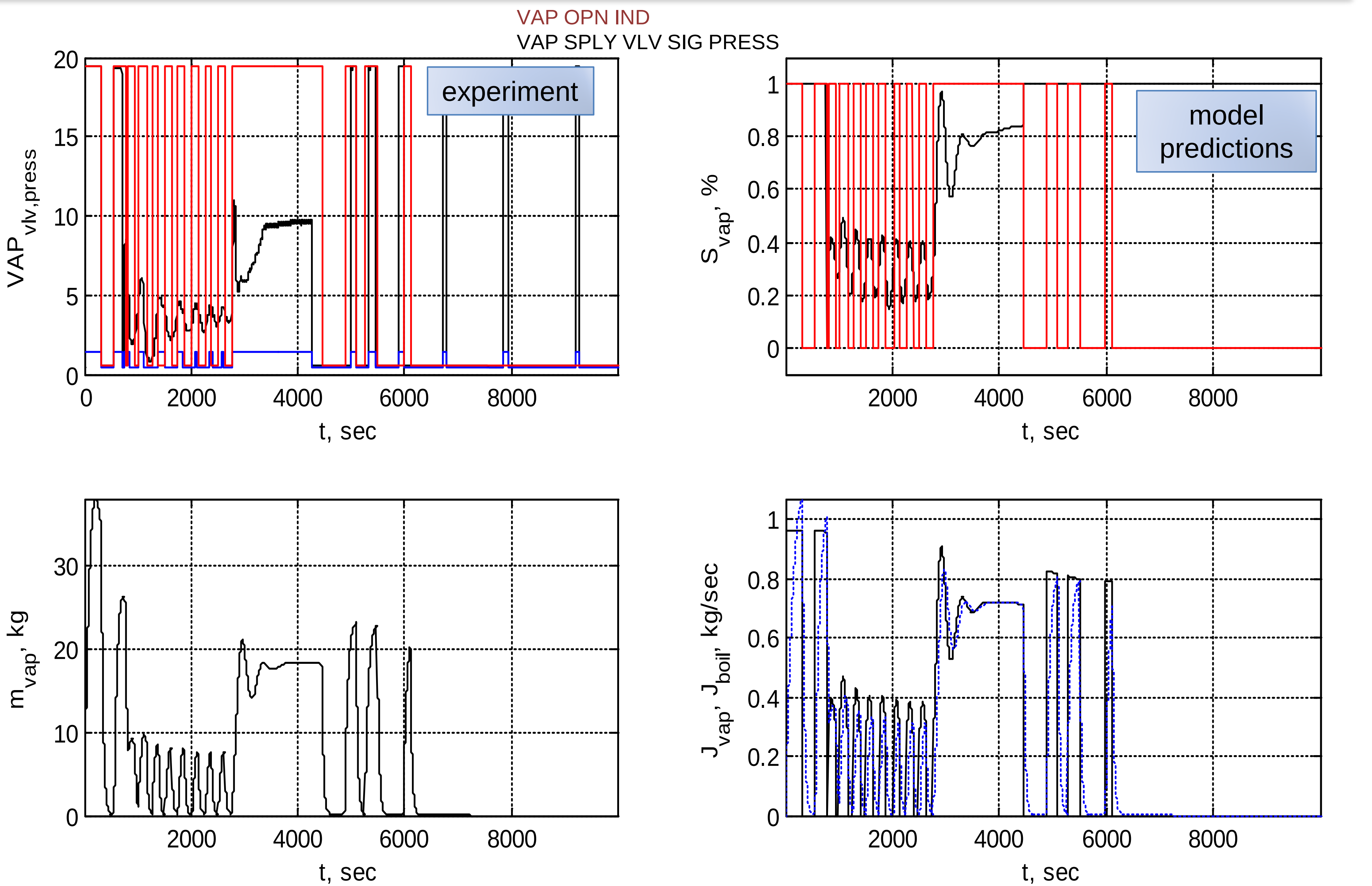

Capabilities: pressure control fault

Experiment

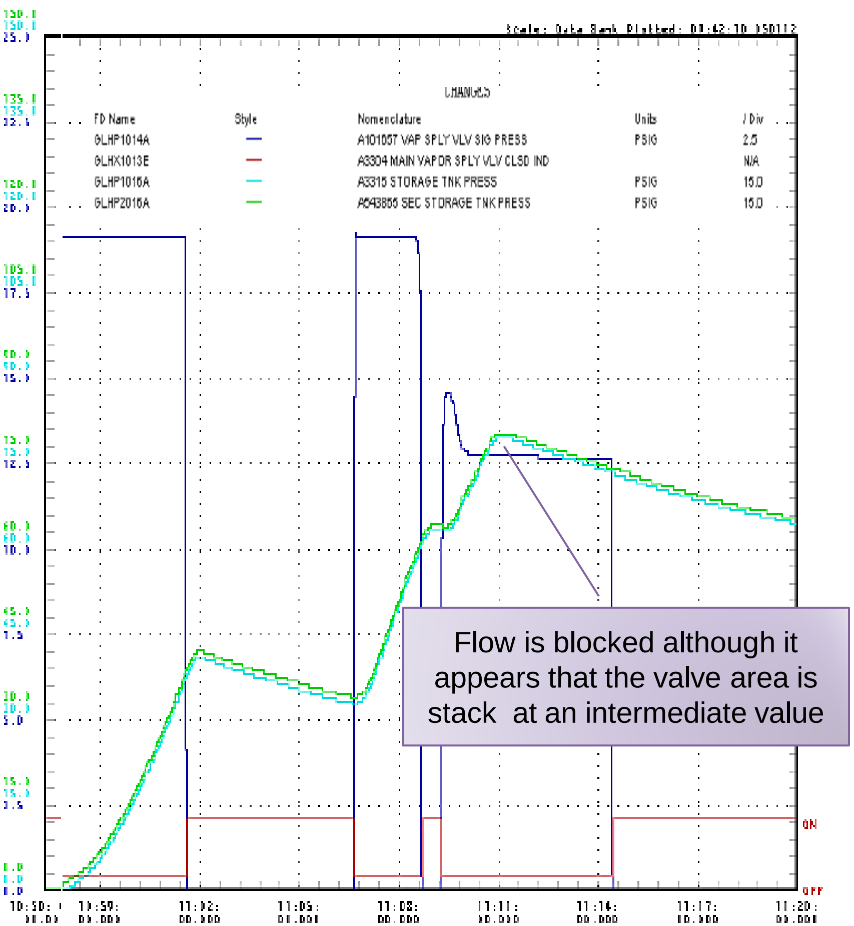

STS-127 A3305 ST Pressure Controller Failure

IPR 127V-119

Simulations

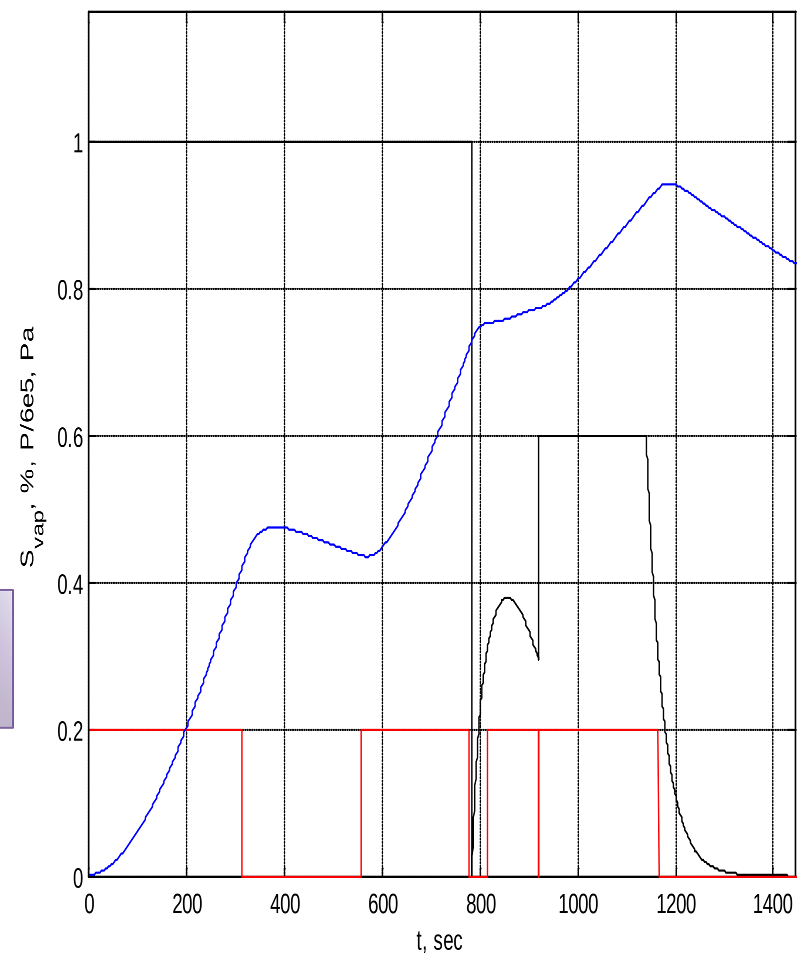

Simultaneous Detection of Multiple Faults

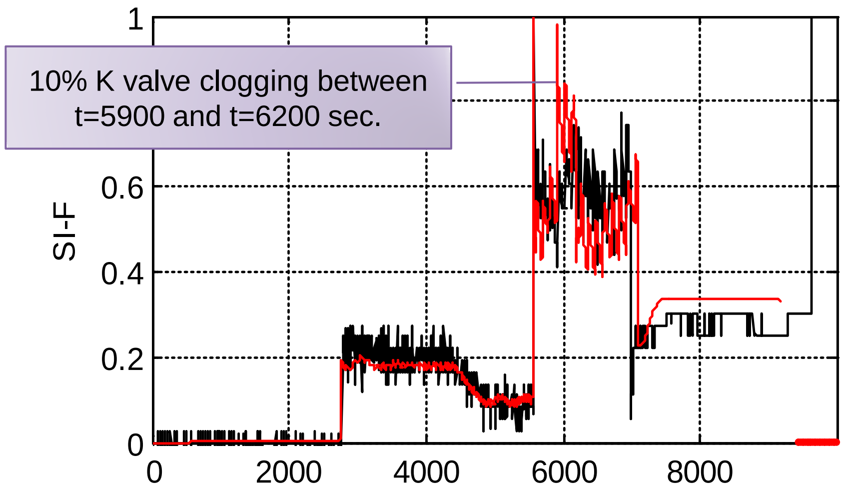

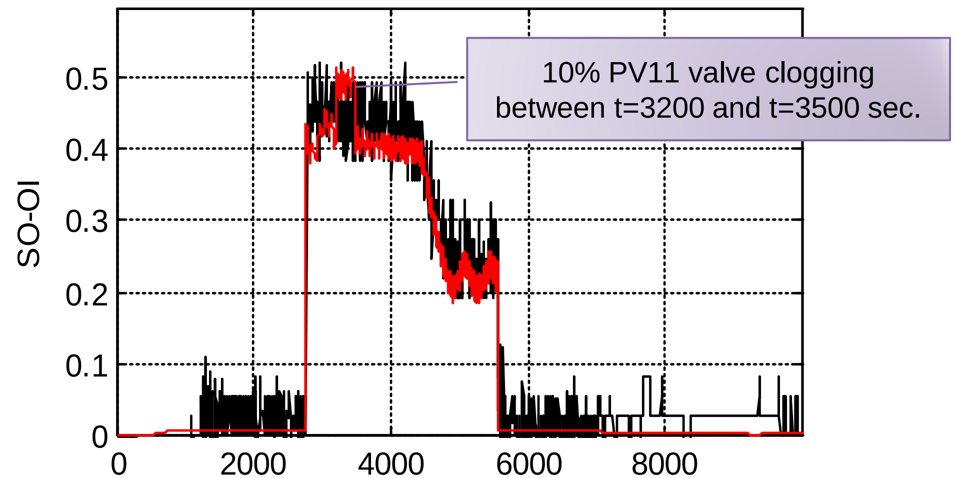

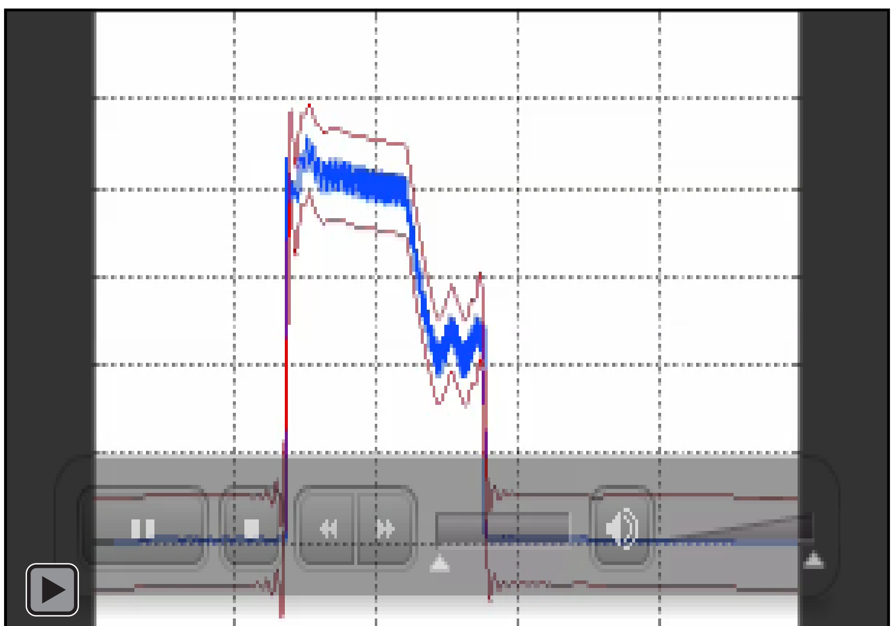

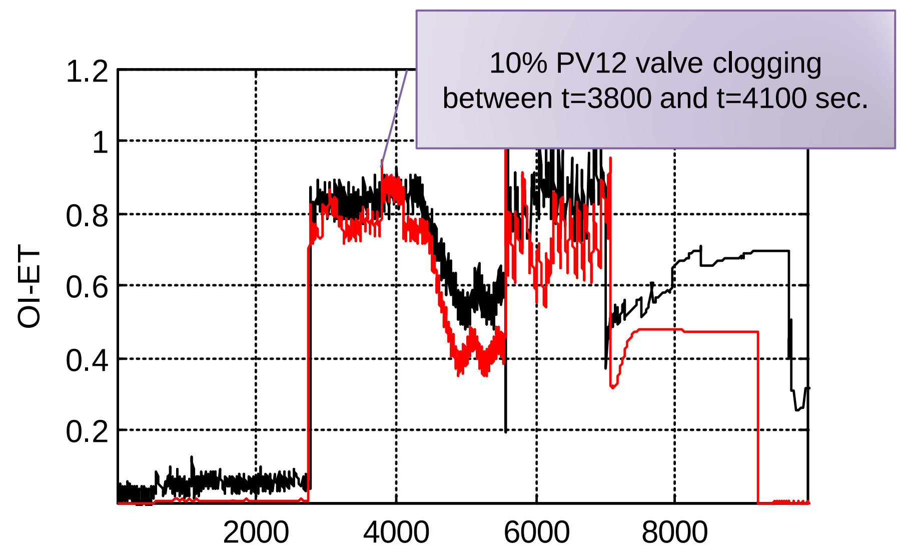

Capabilities: Heat Leak Fault

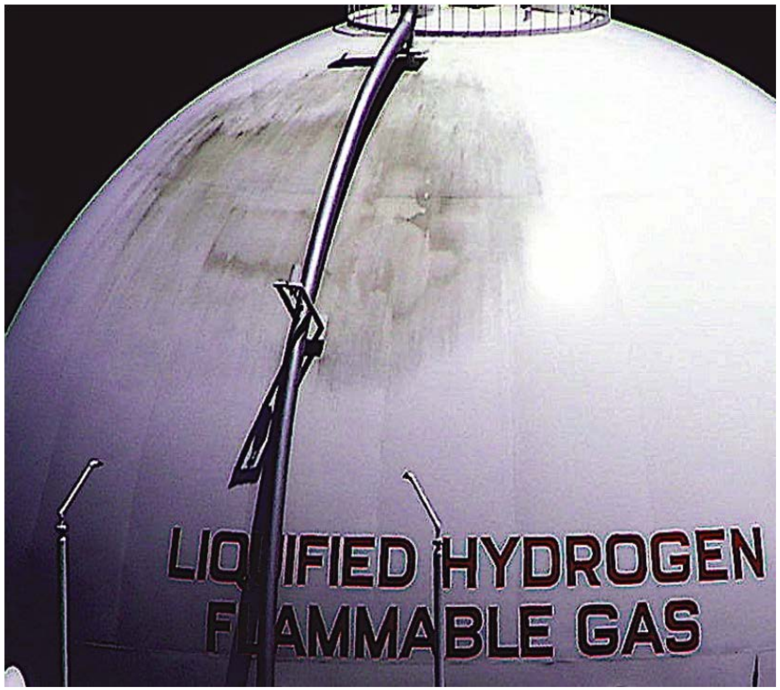

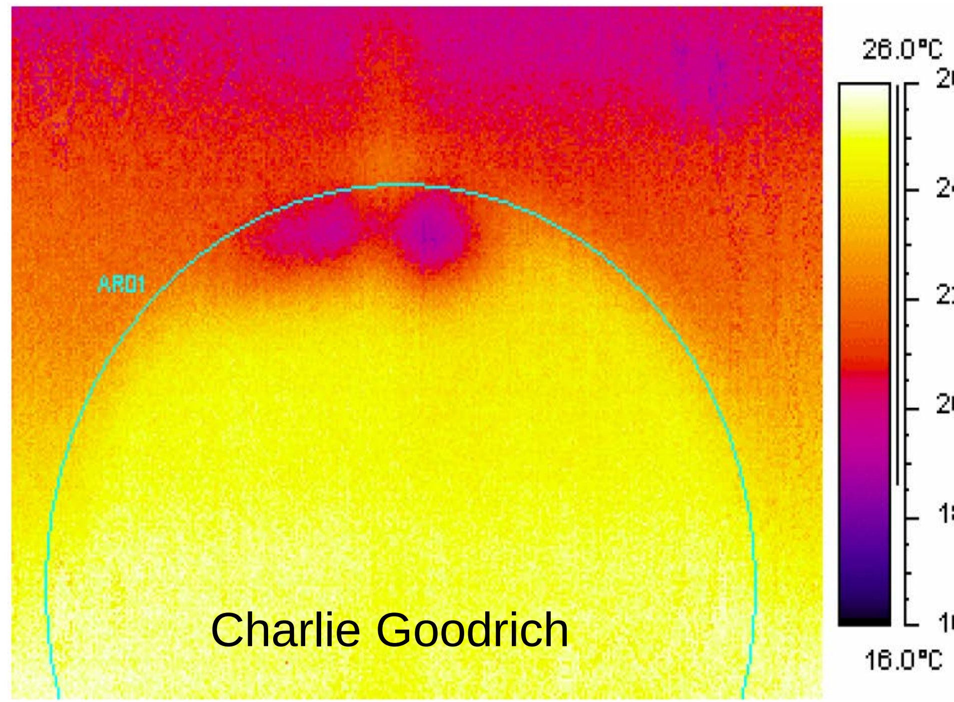

The LC-39 Pad B liquid hydrogen tank experiences on average about 550 gallons per day additional boil-o than the equivalent tank at Pad A. A large mold spot exists on the Pad B tank that is suspected to be the site of a large heat leak. IR camera photography reveals that this spot is indeed much colder than the rest of the tank. Photos of the effected area are shown in Figure.
Mark Nurge, "LC-39B LH2 Tank Thermal Analysis", May 8, 2009

The current model is capable of simulating this nontrivial and important fault

Physics of the Heat and Mass Flow

Main physical processes

1. heat and mass transfer
2. boiling,
3. evaporation-condensation,
4. stratification,
5. natural and forced convection,

We use

Full scale finite element 3D transient turbulent modeling to validate our low-fidelity FD&I models

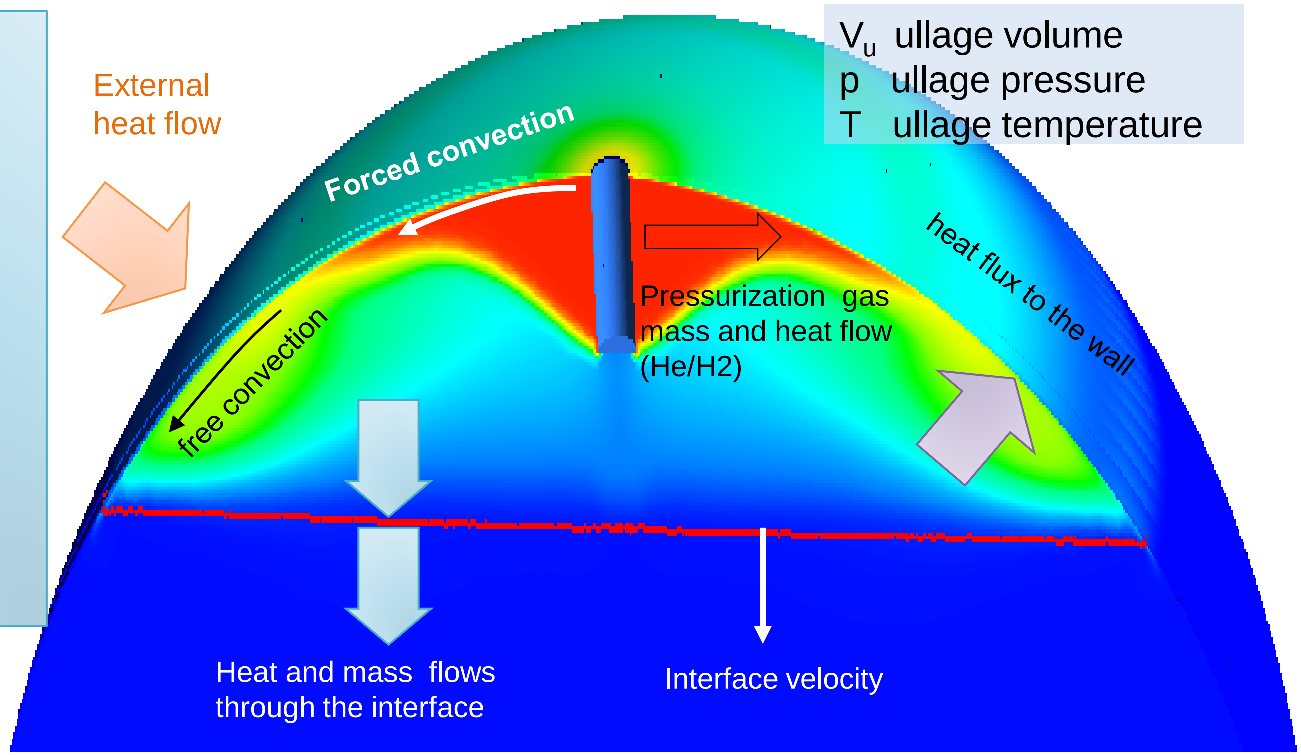

Heat and mass leaks in the vehicle tank appear as small alterations of the heat and mass fluxes in the ullage space. Detection of this faults requires substantially higher fidelity model of the vehicle tank as compared to three-node model discussed earlier. To be able to process signals online such model will have to rely on free convection correlations. Therefore a special attention has to be paid to validation and verification of this model.

Mass and Heat Leaks Modeling

$$\frac{dm}{dt} = J_{in} - J_{out} \qquad T = \frac{pV}{mR}$$

No LN2 leaks $\frac{dV}{dt} \approx 0$

$$\frac{dp}{dt} = -\frac{\gamma p}{V}\frac{dV}{dt} + \frac{\gamma - 1}{V}\left(\dot{Q}_{N2} - \dot{Q}_w\right)$$

$$A d \rho c \cdot \frac{dT_w}{dt} = A h_w (T - T_w) + \dot{Q}_{rad}$$

During the impulse $\dot{Q}_{N2} \gg \dot{Q}_w$
During the relaxation $\dot{Q}_{N2} = 0$

During the heat leak

$$A d \rho c \cdot \frac{dT_w}{dt} = A h_w (T - T_w) + \dot{Q}_{rad} \boxed{+ \dot{Q}_{heat,leak}}$$

During the gas mass leak the wall equation does not change, but

$$\frac{dp}{dt} = \frac{\gamma - 1}{V}\left(\dot{Q}_{N2} - \dot{Q}_w \boxed{- \dot{Q}_{gas,leak}}\right)$$

The problem is to estimate $\dot{Q}_{heat,leak}$ and $\dot{Q}_{gas,leak}$ that will result in the half impulse counting (considering half impulse counting detectable)

LN2 mass leaks

$$\frac{dp}{dt} = \boxed{-\frac{\gamma p}{V}\frac{dV}{dt}} + \frac{\gamma - 1}{V}\left(\dot{Q}_{N2} - \dot{Q}_w\right)$$

Mass or heat leaks could results in the pulses phase shifts or even a different number of pulses during the control time.

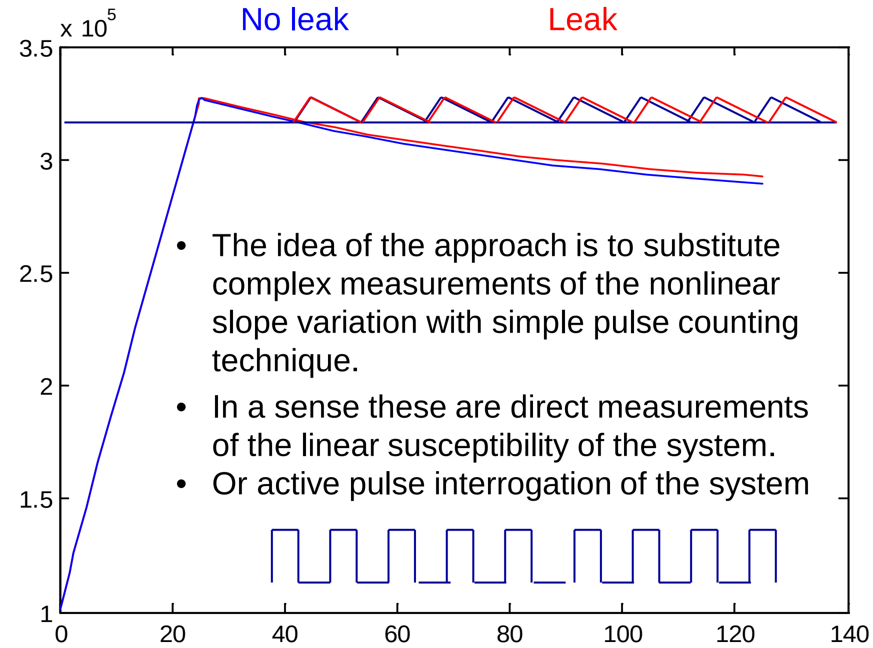

- The idea of the approach is to substitute complex measurements of the nonlinear slope variation with simple pulse counting technique.
- In a sense these are direct measurements of the linear susceptibility of the system.
- Or active pulse interrogation of the system

Modeling of such response imposed on the slow nonlinear variation of the state of the system requires development of a higher fidelity model.

Low Mach Number Approximation

$$\rho_t + \nabla \cdot (\rho\vec{v}) = 0$$
$$(\rho\vec{v})_t + \nabla \cdot (\rho\vec{v} \otimes \vec{v}) + \frac{1}{M^2}\nabla p = \frac{1}{Fr^2}\rho\vec{g}$$
$$(\rho e)_t + \nabla \cdot \big((\rho e + p)\vec{v}\big) = \frac{M^2}{Fr^2}\rho\vec{v}\cdot\vec{g}$$
$$p = (\gamma - 1)\left(\rho e - \frac{1}{2}M^2\rho\vec{v}\cdot\vec{v}\right)$$
$$p = \frac{p'}{p_{ref}};\ \rho = \frac{\rho'}{\rho_{ref}};\ v = \frac{v'}{u_{ref}};\ x = \frac{x'}{l_{ref}};\ t = \frac{t' u_{ref}}{l_{ref}}$$

Eigenvalues of the Jacobian Flux Function

$$f^M = \begin{pmatrix} \rho\vec{v}\cdot\vec{n} \\ \rho\vec{v}\vec{v}\cdot\vec{n} + \frac{1}{M^2}p\cdot\vec{n} \\ (\rho e + p)\vec{v}\cdot\vec{n} \end{pmatrix}$$
$$\vec{v}\cdot\vec{n};\quad \vec{v}\cdot\vec{n} \pm \frac{c}{M};\quad c^2 = \gamma\, p/\rho$$

degenerate when $M = \frac{u_r}{\sqrt{p_r/\rho_r}} \to 0.$

The following expansion is usually introduced:

$$p = p^{(0)} + M^2 p^{(2)}$$

The convective interface velocities v^* are corrected by pressure in the second order:

$$\vec{v}_I = \vec{v}_I^* - \frac{\Delta t}{2}\frac{\nabla p_I^{(2)}}{\rho_I} \qquad \sum_{I\in\mathcal{J}} |I|(\rho h\vec{v})_I \cdot \vec{n} = -\frac{|V|}{\gamma - 1}\frac{dp^{(0)}}{dt}.$$

The Froude number is the ratio of the flow speed to the speed of infinitesimal (incompressible) gravity waves in the same medium: $Fr = u_{ref}/\sqrt{g l_{ref}}$. In fluid dynamics, gravity waves are waves generated in a fluid medium which has the restoring force of gravity or buoyancy

u_{ref} is independent of $c_{ref} = \gamma\sqrt{p_{ref}/\rho_{ref}}$ to ensure that u_{ref} is well defined when $M \to 0$.

u_{ref} is usually chosen from the condition $\rho u_{ref}^2 = l_{ref}\, g\big(\rho(T_u) - \rho(T_w)\big)$

1. Klein R. Semi-implicit extension of a Godunov-type scheme based on low Mach number asymptotics I: One-dimensional flow. Journal of Computational Physics. 1995;121(2):213-237.
2. Schneider T, Botta N, Geratz KJ, Klein R. Extension of Finite Volume Compressible Flow Solvers to Multi-dimensional, Variable Density Zero Mach Number Flows. Journal of Computational Physics. 1999;155(2):248-286.

Energy equation as a divergence constraint

1. Use only 1st approximation $\nabla p^{(0)} = 0$ and neglect completely the momentum equation $(\rho\vec{v})_t + \nabla\cdot(\rho\vec{v}\otimes\vec{v}) + \nabla p^{(2)} = \frac{1}{Fr^2}\rho\vec{g}$

$$\rho_t + \nabla\cdot(\rho\vec{v}) = 0$$
$$(\rho e)_t + \nabla\cdot\big((\rho e + p)\vec{v}\big) = 0$$
$$p = (\gamma - 1)\rho e$$

2. Use the fact that $p^{(0)} = const$ in the whole volume and $\rho e = const$ for each CV:

$$p_t + \gamma p \nabla\cdot\vec{v} = 0 \;\; or \;\; \frac{V_j}{\gamma p}\frac{dp}{dt} = -\frac{dV_j}{dt} + \sum_{k\neq j} u_{kj}S_{kj}$$

3. Integrating over the whole volume we have $\frac{\gamma p}{\gamma-1} = \frac{c_p p}{R} = c_p\rho T$

$$\boxed{\frac{V_j}{\gamma-1}\frac{dp}{dt} = -\frac{\gamma p}{\gamma-1}\frac{dV_j}{dt} + \sum_{k\neq j} c_p T\rho u_{kj}S_{kj} = -\frac{\gamma p}{\gamma-1}\frac{dV_j}{dt} - \dot{Q}_w - \dot{Q}_f + \dot{Q}_{in,v(g)}}$$

1. Kirill's algorithm

System of the ET equations (ULLAGE)

Mass and energy conservation for the bulk gas elements

$$\dot{m}_{i,B} = J_{i+1,B} - J_{i,B} - J_{i+1,BL}, \qquad J = \rho u S, \qquad h = c_p T$$

$$\frac{d}{dt}\sum_{\lambda=v,g} m_{i,B}^{(\lambda)} u_{i,B}^{(\lambda)} = -\dot{W}_{i,B}^{(\lambda)} + \sum_{\lambda=v,g} J_{i+1,B}^{(\lambda)} h_{i+1,B}^{(\lambda)} - \left(J_{i,B}^{(\lambda)} + J_{i,BL}^{(\lambda)}\right) h_{i,B}^{(\lambda)}$$

For the internal boundary layer gas elements

$$\dot{m}_{i,L}^{(\lambda)} = J_{i-1,L}^{(\lambda)} - J_{i,L}^{(\lambda)} + J_{i,BL}^{(\lambda)}$$

$$\frac{d}{dt}\sum_{\lambda=v,g} m_{i,L}^{(\lambda)} u_{i,L}^{(\lambda)} = \dot{Q}_{i,e}^{(\lambda)} - \dot{W}_{i,L}^{(\lambda)} + \sum_{\lambda=v,g}\left(J_{i-1,L}^{(\lambda)} h_{i-1,L}^{(\lambda)} - J_{i,L}^{(\lambda)} h_{i,L}^{(\lambda)}\right) + J_{i,BL}^{(\lambda)} h_{i,B}^{(\lambda)}$$

For the lowest horizontal vapor layer

$$\dot{m}_{1,B}^{(v)} = J_{2,B}^{(v)} - J_{1,L}^{(v)} + J_{ev}; \qquad \dot{m}_{1,B}^{(g)} = J_{2,B}^{(g)} - J_{1,L}^{(g)}$$

$$\frac{d}{dt}\sum_{\lambda=v,g} m_{1,B}^{(\lambda)} u_{1,B}^{(\lambda)} = \dot{Q}_v - \dot{W}_{1,B} + \sum_{\lambda=v,g}\left(J_{2,B}^{(\lambda)} h_{2,B}^{(\lambda)} - J_{1,B}^{(\lambda)} h_{1,B}^{(\lambda)}\right) + J_{ev} h_{vs}$$

For the upper horizontal vapor layer

$$\dot{m}_{n,B}^{(\lambda)} = J_{n-1,L}^{(\lambda)} - J_{n,B}^{(\lambda)} + J_{\lambda,e}$$

$$\frac{d}{dt}\sum_{\lambda=v,g} m_{n,B}^{(\lambda)} u_{n,B}^{(\lambda)} = \dot{Q}_{top} - \dot{W}_{n,B} + \sum_{\lambda=v,g}\left(J_{n-1,B}^{(\lambda)} h_{n-1,B}^{(\lambda)} - J_{n,B}^{(\lambda)} h_{n,B}^{(\lambda)}\right) + J_{\lambda,e} h_{\lambda,e}^{(\lambda)}$$

Fluxes between Control Volumes are calculated in low Mach approximation

$$\frac{V_j}{\gamma p}\frac{dp}{dt} = -\frac{dV_j}{dt} + \sum_{k\neq j} u_{kj} S_{kj}$$

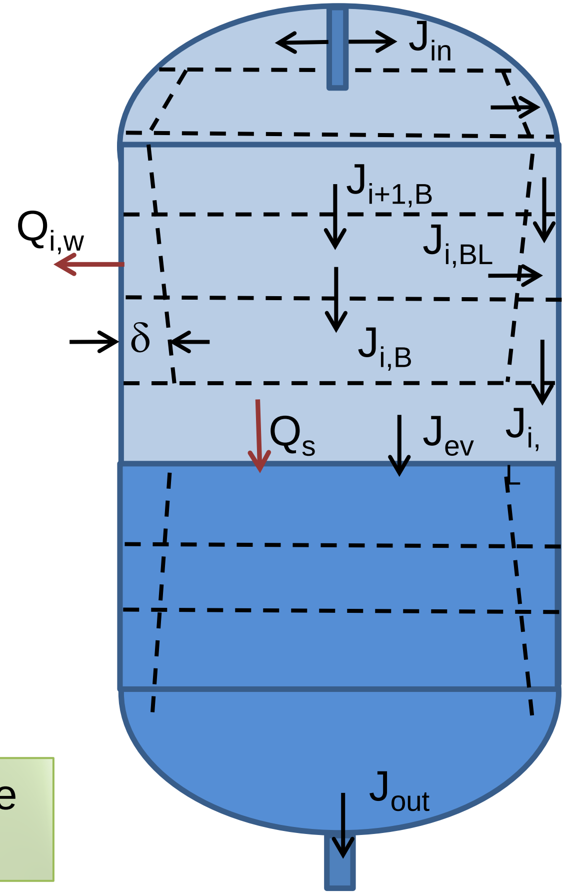

The system is closed using equations of state for ideal gas. The real tank geometry was used.

Interface: balance

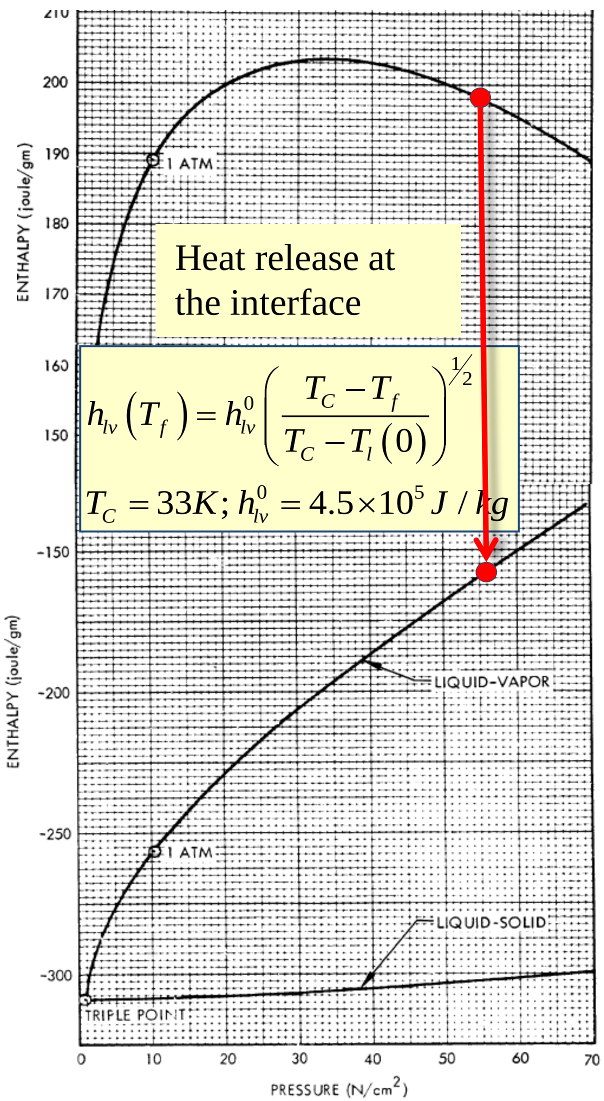

$$\dot{Q}_v - \dot{Q}_l + J_{lv}h_{lv} + J_{lv}c_p\left(T_u - T_s\right)\left(\dot{Q}_l > \dot{Q}_v\right) = 0$$

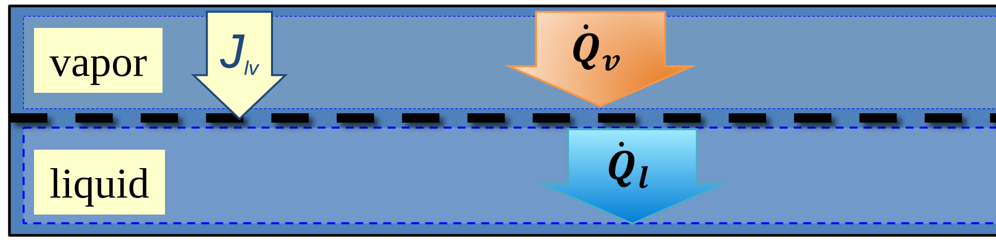

1. Under non-equilibrium conditions (blow-down) there is continuous condensation/evaporation flow to/from the surface;
2. There is no accumulation of the mass;
3. The heat released ($J_{lv}h_{vs}$) can not be accumulated at the interface and is balanced by heat flow to/from interface on liquid and vapor sides;
4. The heat flow in vapor (liquid) phases are defined as follows

$$\dot{Q}_{v(l)} = \dot{Q}^{(cv)}_{v(l)} + \dot{Q}^{(cd)}_{v(l)} = A\alpha_{v(l)}\left(T_s - T_{v(l)}\right) + \dot{Q}^{(cd)}_{v(l)}$$

5. During prepress and repress $T_g > T_s > T_L = 20.4K$ and convective heat transfer can be neglected

Heat conduction

Heat conduction eq. with a given heat source and surface temperature

$$(1)\quad \begin{cases} \rho c \dfrac{\partial u}{\partial t} = \kappa \dfrac{\partial^2 u}{\partial x^2} + Q(x,t) \\ u(x,0) = 0 \\ u(0,t) = T_s(t) \end{cases}$$

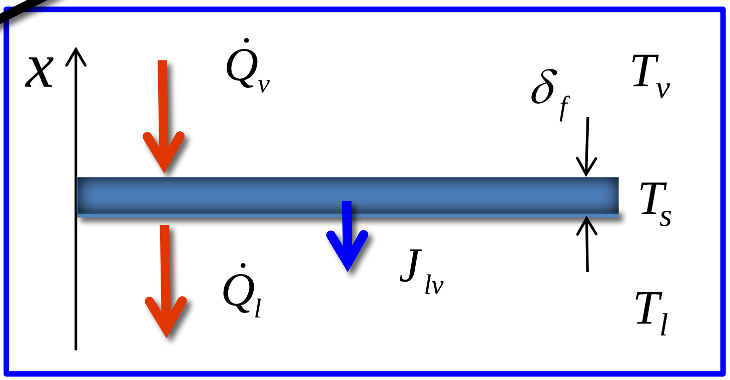

$$\boxed{\dot{Q}_v - \dot{Q}_l = J_{ev}\left(h_{vs} - h_{ls}\right)}$$

General solution

$$(2)\quad u(x,t) = u_1(x,t) + u_2(x,t) = \left[\chi = (\kappa/\rho c)\right] =$$

$$\frac{x}{2\sqrt{\pi\chi}} \int_0^t \frac{T_s(\tau)}{(t-\tau)^{3/2}} e^{-\frac{x^2}{4\chi(t-\tau)}} d\tau + \frac{1}{2\sqrt{\pi\chi}} \int_0^\infty d\xi \int_0^t \frac{Q(\xi,\tau)d\tau}{\sqrt{t-\tau}} \left\{ e^{-\frac{(x-\xi)^2}{4\chi(t-\tau)}} - e^{-\frac{(x+\xi)^2}{4\chi(t-\tau)}} \right\}$$

Surface temperature gradient for uniform heat source

$$(3)\quad \left.\frac{\partial u(x,t)}{\partial x}\right|_{x=0} = -\frac{1}{\sqrt{\pi\chi_v}} \int_0^t \frac{\partial T_s(\tau)}{\partial \tau} \frac{d\tau}{\sqrt{t-\tau}} + \frac{1}{\sqrt{\pi\chi_v}} \int_0^t \frac{\partial T_v(\tau)}{\partial \tau} \frac{d\tau}{\sqrt{t-\tau}} - \frac{1}{\sqrt{\pi\chi_l}} \int_0^t \frac{\partial T_s(\tau)}{\partial \tau} \frac{d\tau}{\sqrt{t-\tau}}$$

Optimal grid

Heat conduction at the interface can be found by solving numerically HCE

$$\dot{Q}^{cd}_{l(v)} \approx \left[\frac{\kappa_l \left(T_1 - T_0\right)}{h_{1/2}} - h_0 c_{l(v)} \rho_{l(v)} \frac{dT_0}{dt} \right],$$

$$h_i c_{l(v)} \rho_{l(v)} \frac{dT_i}{dt} = \kappa_{l(v)} \left[\frac{\left(T_{i+1} - T_i\right)}{h_{i+1/2}} - \frac{\left(T_i - T_{i-1}\right)}{h_{i-1/2}} \right], \quad i = 1, 2, \ldots, i-1$$

$$T_0\left(t\right) = T_s\left(t\right), \quad T_i\left(0\right) = T_L, \quad T_n = T_L$$

on the optimal grid [1-3]

$$h_0 = \frac{h_{\min}}{1 + \exp\left(\pi / \sqrt{n}\right)}, h_{1/2} = h_{\min} = \sqrt{\frac{\kappa_l t_{\min}}{c_l \rho_l}}, h_{i+1/2} = h_{i-1/2} \exp\left(\pi / \sqrt{n}\right), h_i = \sqrt{h_{i+1/2} h_{i-1/2}}.$$

$$\frac{\exp\left(\pi\sqrt{n}\right) - 1}{\exp\left(\pi / \sqrt{n}\right) - 1} > \sqrt{\frac{t_{\max}}{t_{\min}}} \geq 100 \qquad n \approx 8$$

[1] D. Ingerman, V. Druskin, and L. Knizhnerman, “Optimal finite difference grids and rational approximations of the square root”, I. Elliptic problems. Commun. Pure Appl. Math., 53, pp. 1039–1066 (2000).
[2] V. Druskin, Spectrally optimal finite difference grids in unbounded domains. Schlumberger-Doll Research Notes, pages EMG–002–97–22, 1997.
[3] V. Druskin and S. Moskow, ”Three-point finite difference schemes, Pad´e and the spectral Galerkin method”, I. One-sided impedance approximation., Math. Comput., 71, pp. 995–1019 (2001).'

Model validation using LO2 Shuttle data

- To detect heat and mass leaks in the GN2 vehicle (storage) tank we propose to use/modify/upgrade standard technique verified and validated for LH2 and LO2 tanks
- The technique is using calibrated pulses of hot gas introduced in the pressurized tank every time when pressure goes below preset limit.
- Validation of the model:
  - o The top figure shows comparison of the model predictions (blue) with experimental data (green) for LO2 tank during countdown before physics model is improved and validated;
  - o The middle figure shows high-fidelity model used for validation;
  - o The bottom figure shows performance of the model after its validation and correction using improved:
    - material properties;
    - GHe pressurization pulse dynamics;
    - free convection correlations at the wall.'''

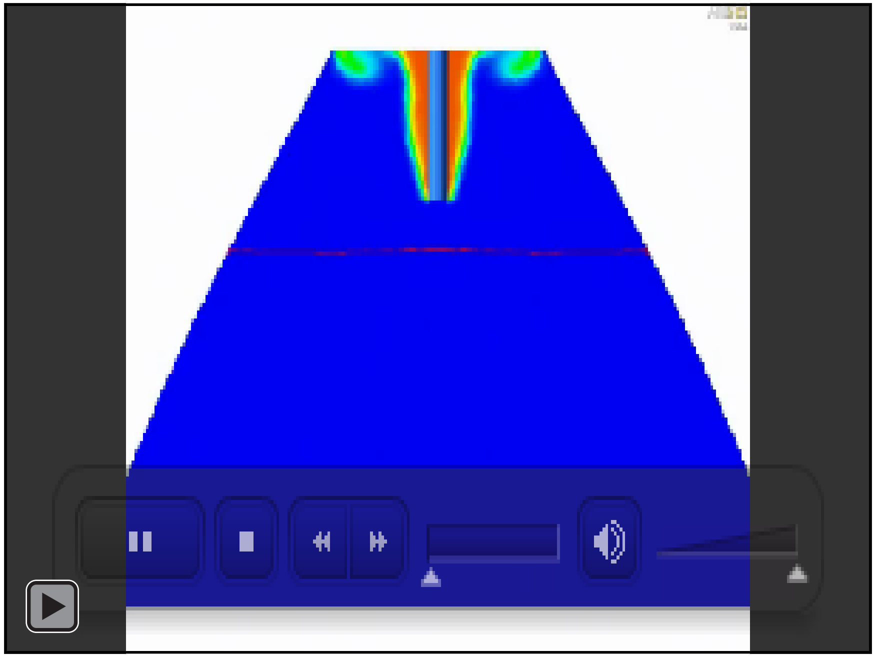

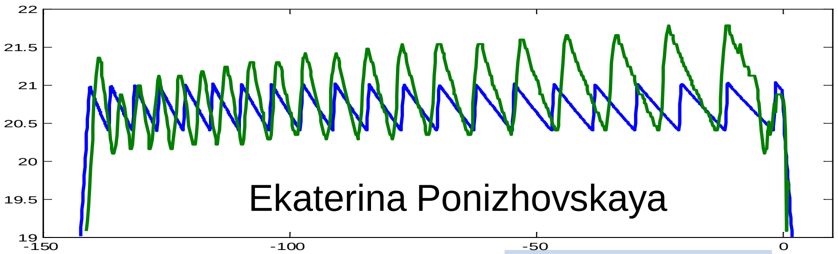

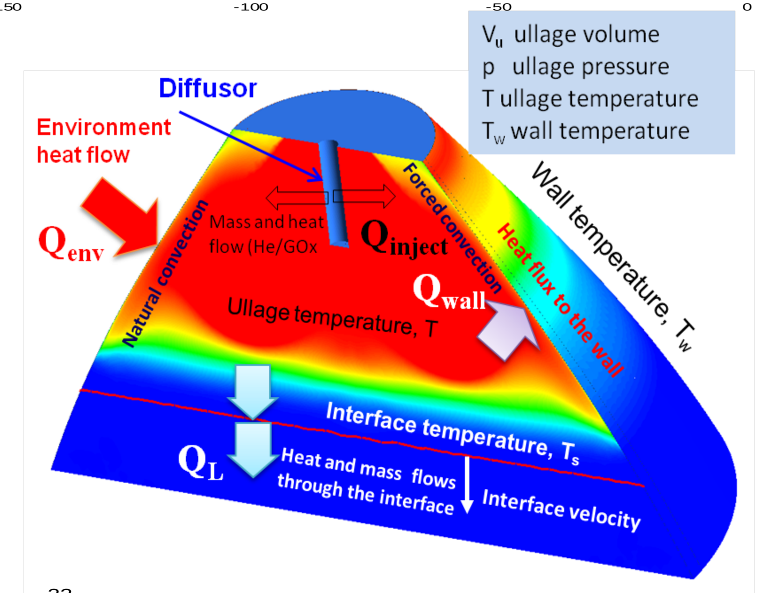

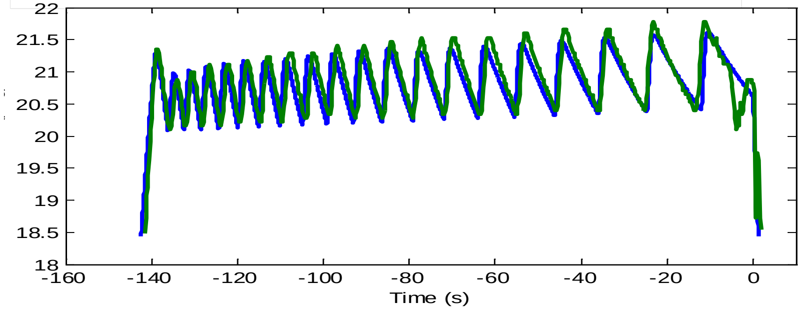

Model validation using LH2 Shuttle data

Ekaterina Ponizhovskaya

Model validation using Shuttle data for LH2 ET
This test demonstrates that the model (blue) can accurately reproduce both experimental (green) pressure and temperature time series data for

- Prepress
- Pulse dynamics during prepress
- Repress
- Earlier in flight dynamics

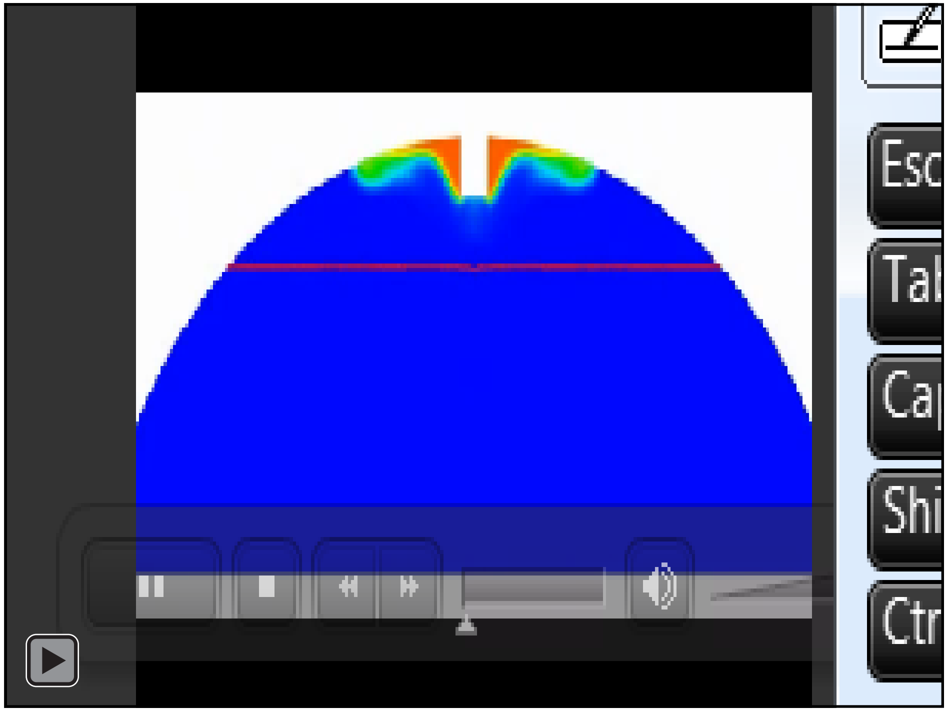

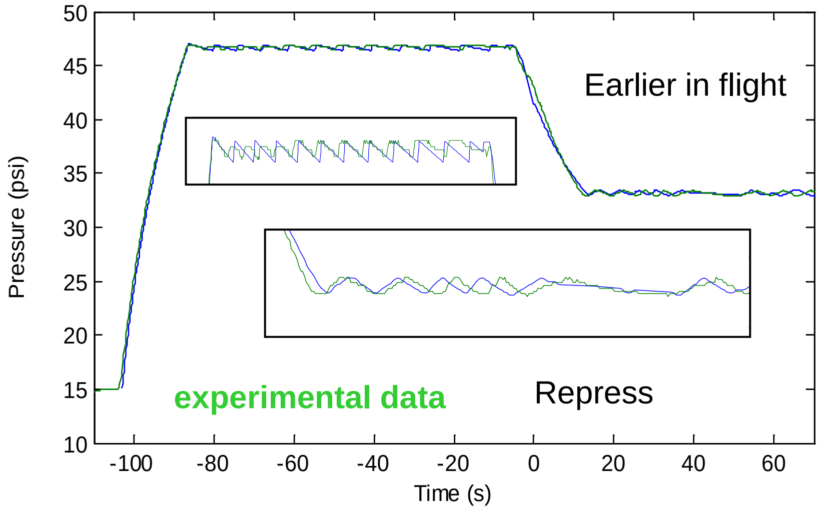

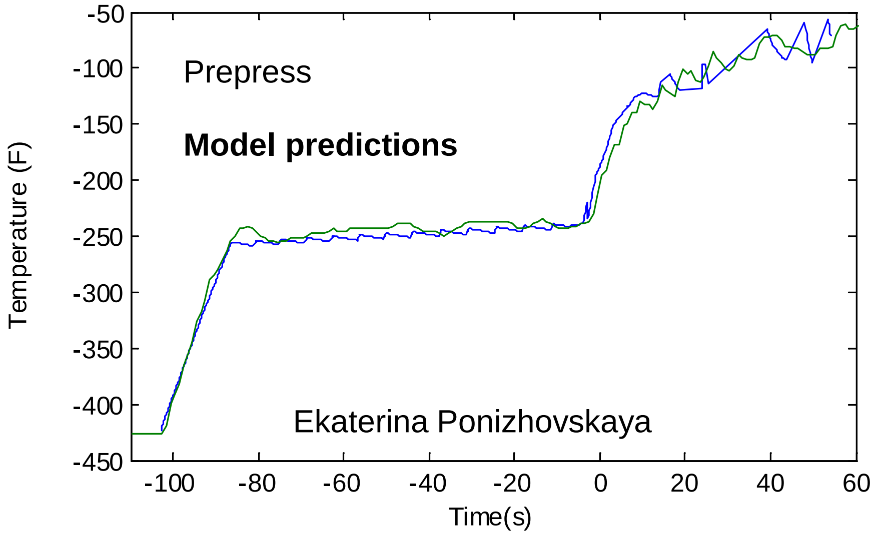

Heat leak in the tank

Ekaterina Ponizhovskaya

Tank volume 2000 Gal;
Temperature of GN2 flow is 572R;
GN2 pulses had duration 0.5s,
flow rate 0.5lb/s, shark fin shape

- In this test we first check the dispersion of the pulses frequency as a function of the pulses mass flow dispersion. It is shown that to detect 1 extra pulse the deviation of the mass flow rate should be kept within few %

- In the next test a continuous heat leaks of various level are applied to the patch with area $1m^2$. It is shown that the heat leak 1kW can be detected (given condition above on the deviation of the pulse mass flow rate)

Ekaterina Ponizhovskaya

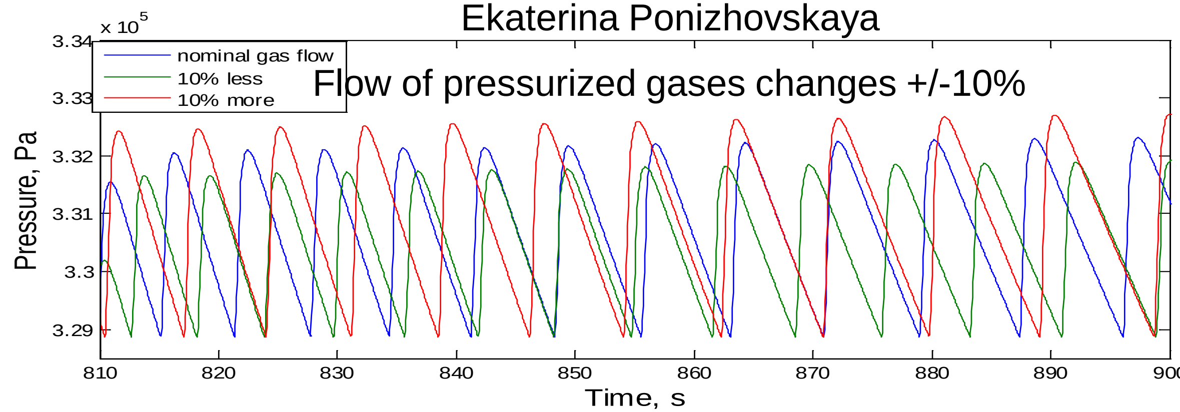

Pressure with a heat leaks in the patch area $1m^2$.
The leaks 0, 50, 100, 500 W/m^2

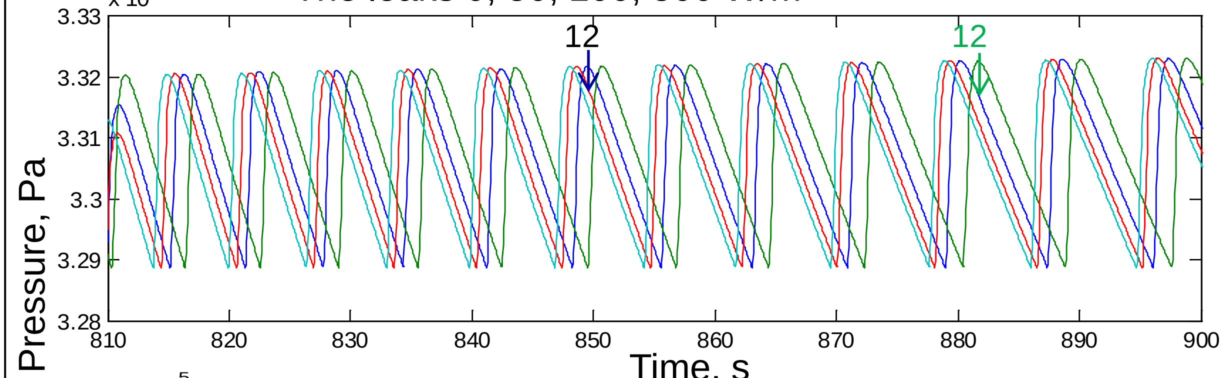

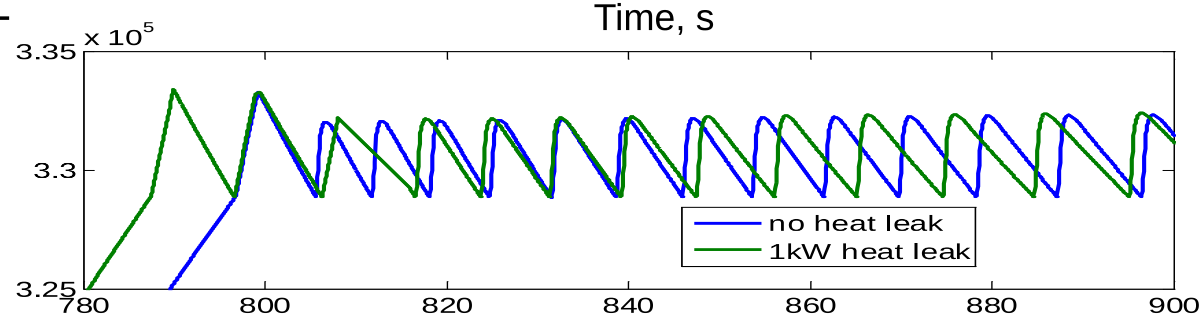

Gas and Liquid Leaks in the Tank

Ekaterina Ponizhovskaya

Tank volume 2000 Gal;
Temperature of GN2 flow is 572R;
GN2 pulses had duration 0.5s,
flow rate 0.5lb/s, shark fin shape

- In the 3rd test we demonstrate liquid leaks with mass flow rate 0.5 kg/s (0.116 Gal/s) can be detected
- In the final test it is shown that the gas leak with mass flow rate 0.01 kg/s can be detected

Liquid leak LN2

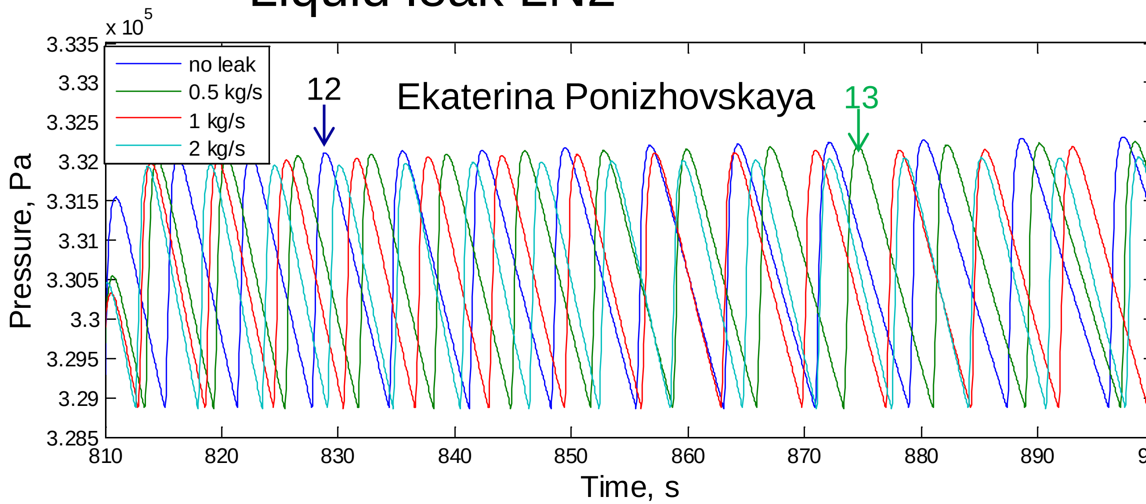

Gas leak GN2

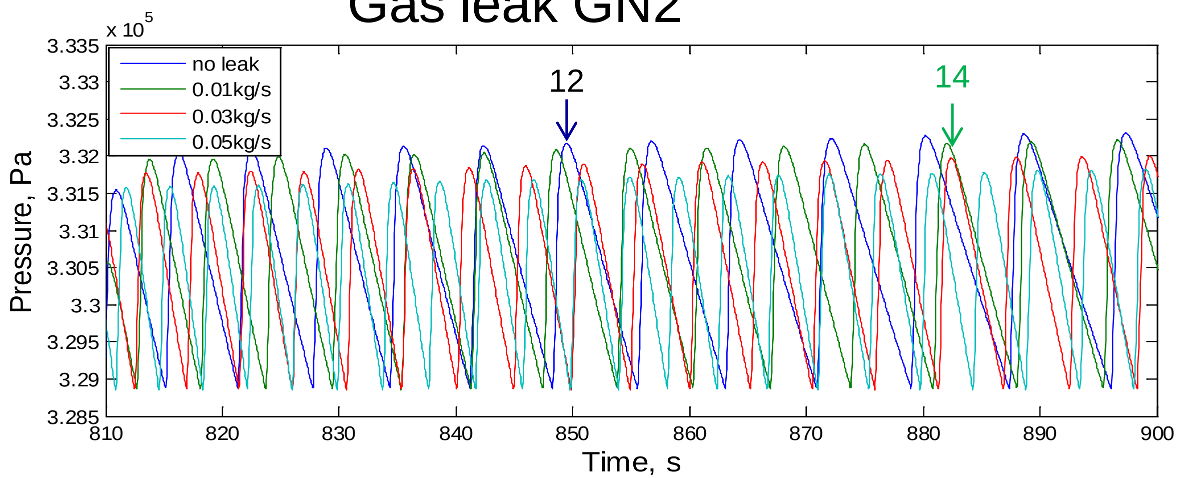

Stratification and Chilldown (Nodes)

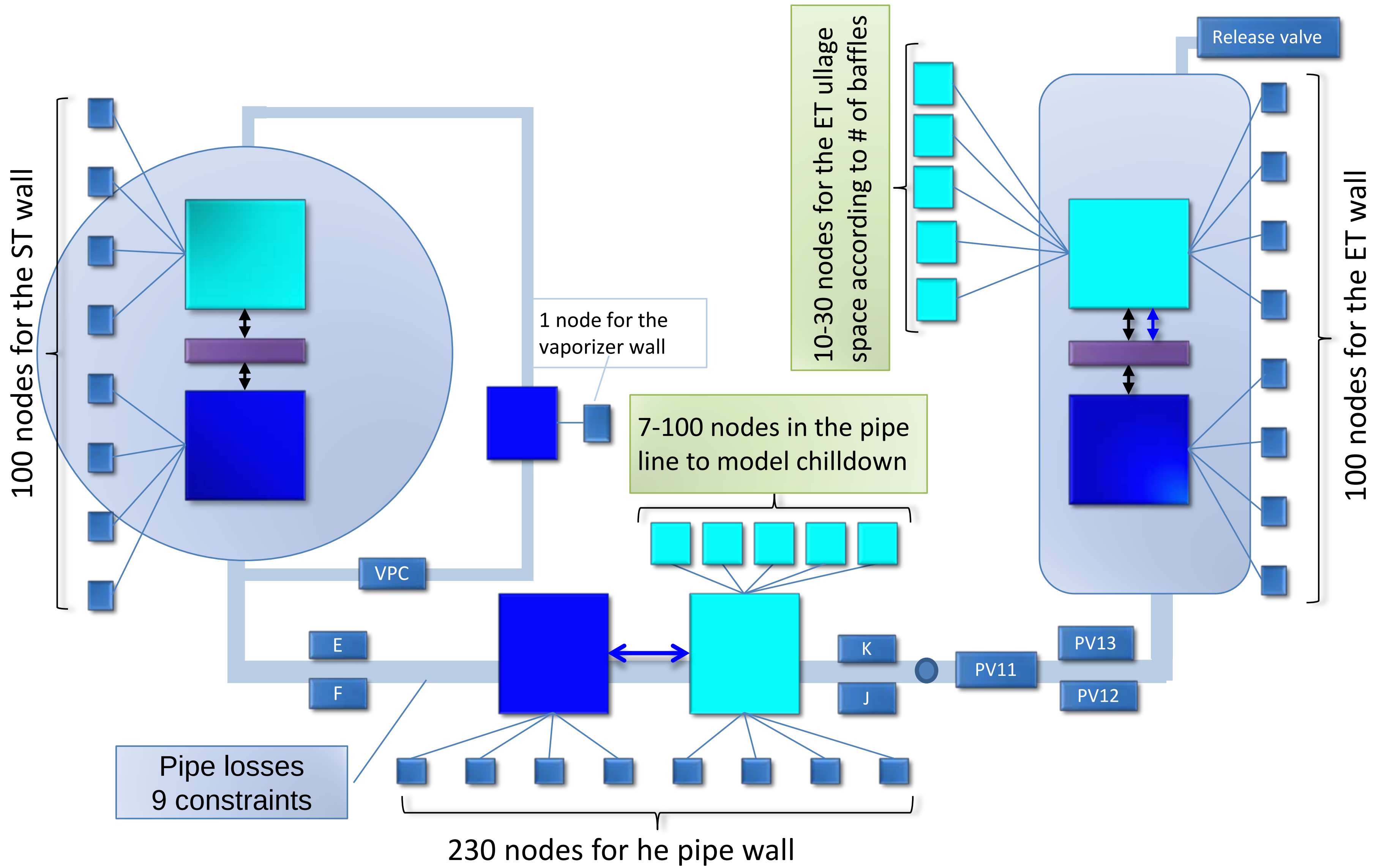

Conclusions

- Model of the LH2 loading operation was developed and validated
  - Pressure oscillations and losses in transfer line can be accurately reproduced
- The model capability of detecting multiple faults were demonstrated including:
  - Vaporizer Pressure Control faults
  - Simultaneous valve clogging in transfer Line
  - Mass and Heat Leaks in the Vehicle tank
- Work in progress:
  - Chilldown model of the transfer line coupled to stratification model of the vehicle tank